*Journal of Neurocytology* **24**, 409–433 (1995)

# Differential distribution of N-acetylaspartylglutamate and N-acetylaspartate immunoreactivities in rat forebrain

JOHN R. MOFFETT* and M.A.A. NAMBOODIRI

*Department of Biology, Georgetown University, 37th & O Sts N.W., Washington, DC 20057-1028, USA*

Received 8 November 1994; revised 6 January 1995; accepted 25 January 1995

## Summary

Contradictory immunohistochemical data have been reported on the localization of N-acetylaspartylglutamate in the rat forebrain, using different carbodiimide fixation protocols and antibody purification methods. In one case, N-acetylaspartylglutamate immunoreactivity was observed in apparent interneurons throughout all allocortical and isocortical regions, suggesting possible colocalization with GABA. In another case, strong immunoreactivity was observed in numerous pyramidal cells in neocortex and hippocampus, suggesting colocalization with glutamate or aspartate. Reconciling these disparate findings is crucial to understanding the role of N-acetylaspartylglutamate in nervous system function. Antibodies to N-acetylaspartylglutamate and a structurally related molecule, N-acetylaspartate, were purified in stages, and their cross-reactivities with protein conjugates of N-acetylaspartylglutamate and N-acetylaspartate were monitored at each stage by solid-phase immunoassay. Reduction of the cross-reactivity of the anti-N-acetylaspartylglutamate antibodies to N-acetylaspartate-protein conjugates to about 1% eliminated significant staining of most pyramidal neurons in the rat forebrain. Utilizing highly purified antibodies, the distributions of N-acetylaspartylglutamate and N-acetylaspartate were examined in several major telencephalic and diencephalic regions of the rat, and were found to be distinct. N-acetylaspartylglutamate-immunoreactivity was observed in specific neuronal populations, including many groups thought to use GABA as a neurotransmitter. Among these were the globus pallidus, ventral pallidum, entopeducular nucleus, thalamic reticular nucleus, and scattered non-pyramidal neurons in all layers of isocortex and allocortex. N-acetylaspartate-immunoreactivity was more broadly distributed than N-acetylaspartylglutamate-immunoreactivity in the rat forebrain, appearing strongest in many pyramidal neurons. Although N-acetylaspartate-immunoreactivity was found in most neurons, it exhibited a great range of intensities between different neuronal types.

## Introduction

N-acetylaspartylglutamate (NAAG) is a nervous system specific dipeptide which may be involved in excitatory neurotransmission through NMDA-type glutamate receptors (Westbrook *et al.*, 1986; Sekiguchi *et al.*, 1992), and in neurotransmitter release modulation (Galli *et al.*, 1991; Puttfarcken *et al.*, 1993). A structurally related nervous system specific compound which is found in very high concentrations in the brain is N-acetylaspartate (NAA). Due to its exceptionally high concentration, and the presence of acetyl group protons, NAA generates the major signal in water-suppressed proton magnetic spectrograms of human brain (Birken & Oldendorf, 1989). Deficiency in the activity of the enzyme required for the deacetylation of NAA, aspartoacylase, is associated with Canavan disease, a degenerative leukodystrophy in infants and children (Hagenfeldt *et al.*, 1987; Matalon *et al.*, 1988). Despite their presence in the brain in high concentrations, the specific functions subserved by these two compounds remain elusive. Accurate identification of NAAG and NAA containing neurons in CNS will be essential information for neuroscientists and clinicians studying their functions in health and disease.

A recent immunohistochemical investigation by Tsai and colleagues (1993) on the localization of NAAG in the rat forebrain reported that most cortical and hippocampal pyramidal cells contained high levels of immunoreactivity for NAAG. These results were interpreted to indicate the presence of NAAG in most rat forebrain glutamatergic systems, suggesting a link between NAAG and excitatory, glutamate-based

*To whom correspondence should be addressed.

0300–4864/95 

neurotransmission in rat cortex. Other immunohistochemical studies, however, had demonstrated a lack of NAAG-immunoreactivity (NAAG-IR) in cortical and hippocampal pyramidal cells in the rat, and instead, noted the presence of NAA-immunoreactivity (NAA-IR) in these cells (Moffett *et al.*, 1991a, 1993). These studies reported the presence of NAAG-IR predominantly in apparent interneurons in rat telecephalon, suggesting a link with inhibitory, GABA-type neurotransmission. Because different fixation techniques and antibody purification methods were employed by the two groups, the methods are a potential source of the observed discrepancies.

The immunohistochemical localization of small molecules which contain only carboxyl groups as reactive sites for covalent bond formation can be accomplished by using water soluble carbodiimides as both coupling reagents for antigen production, and fixative reagents for the cellular localization of the molecule (Goodfriend *et al.*, 1964; Kendall *et al.*, 1971; Willingham & Yamada, 1979; Bauminger & Wilcheck, 1980; Moffett *et al.*, 1993). The covalent attachment of small molecules, such as NAAG, to protein carriers is necessary to induce a strong immune response and generate antibodies, while the covalent coupling of the molecule to tissue proteins during fixation is necessary for their accurate localization by immunohistochemistry. The present study addresses problems associated with the immunohistochemical localization of NAAG and NAA in the rat forebrain. Antibodies to NAAG and NAA were purified by both positive-affinity chromatography, and negative-affinity adsorption, and their cross-reactivities with protein conjugates of NAAG and NAA were monitored by solid-phase immunoassay.

Based upon solid-phase immunoassay results with the anti-NAAG antibodies it was determined that cross-reactivity to NAA-protein conjugates was reduced from over 20% after affinity purification to approximately 1% after adsorption with protein-coupled NAA. Comparisons were made between the immunohistochemical signal provided by the one-stage purified anti-NAAG antibodies and the two-stage purified antibodies to NAA and NAAG. It was observed that significant staining of most pyramidal cells in the rat cortex was associated with the one-stage purified anti-NAAG antibodies, and both types of anti-NAA antibodies, but not with the two-stage purified antibodies to NAAG. This suggests that pyramidal cell staining was a function of antibody binding to protein-coupled NAA, not protein-coupled NAAG. The two-stage purified antibodies to NAAG and NAA were used to localize these molecules in rat brain tissue fixed by the enhanced carbodiimide method (Moffett *et al.*, 1993). Using the described antibody purification and fixation methods, differential NAAG and NAA staining patterns were observed in the rat forebrain. The differences observed in the staining patterns were consistent with the possibility that the immunoreactivity observed in most pyramidal and granule cells by Tsai and colleagues (1993) may have been due to antibody cross-reactivity with protein-coupled NAA. The two-stage purified NAAG and NAA antibodies were used to analyse the distributions of these two brain-specific compounds in carbodiimide-fixed brain tissue sections. A brief description is given of their comparative distributions in selected areas of the rat forebrain, and problems associated with NAAG and NAA immunohistochemistry are discussed.

## Materials and methods

Chemicals and bovine skeletal muscle actin were purchased from Sigma Chemical Co. (St. Louis, MO). Solutions were prepared with deionized water. Normal goat serum (NGS), horseradish peroxidase (HRP) labelled avidin-biotin complex, and biotinylated secondary antibody reagents were purchased from Vector Labs (Vectastain Elite; Burlingame, CA). HRP-labelled goat-anti-rabbit antibodies were purchased from Kirkegaard and Perry (Gaithersburg, MD). The quantities of all protein-hapten conjugates described in the text refer to protein weight.

### *Antibody production*

The polyclonal antibodies to NAAG and NAA were produced in New Zealand white rabbits ($n = 3$ NAAG, $n = 1$ NAA, Hazleton Biologics; Lenexa, KS) as previously described for NAAG (Moffett *et al.*, 1994). Immunizations were administered on a trimonthly schedule with injections of either carrier-bound NAAG or carrier-bound NAA. Carriers were alternated by using two different proteins, and colloidal gold particles for different injections. The two protein carriers were injected alternately, between gold-adsorbed NAAG or NAA immunizations. The protein based antigens were produced by mixing 10 mg of either limulus hemocyanin or bovine thyroglobulin with 5 mg of NAAG or NAA and 200 mg of carbodiimide (1-ethyl-3[3-dimethylaminopropyl] carbodiimide hydrochloride; EDAC) in 10 ml of water. The solutions were adjusted to pH 6.5 with NaOH and agitated by rotation for 30 min at room temperature. Conjugates were dialysed against cold PBS (10 mM $Na_2HPO_4$, 150 mM NaCl, pH 7.4), and stored frozen until used. For initial immunizations, 500 µg of either NAAG-thyroglobulin or NAA-thyroglobulin, each in 500 µl of PBS, were emulsified with 500 µl of TiterMax adjuvant (Vaxcel; Norcross, GA), and injected subcutaneously at several sites into the respective rabbits. The second immunization was given 3 months later using gold particle adsorbed NAAG or NAA prepared by adding 2 mg of either hapten to 500 µl purified water (Shiosaka *et al.*, 1986). The pH was adjusted to 7.4 with NaOH, and the mixtures were each added to 500 µl of a colloidal gold solution (15 mM particle size; EY Lab., San Mateo, CA). The mixtures were emulsified with 1 ml of Freund's incomplete adjuvant (Gibco Labs; Grand Island, NY) and injected subcutaneously at multiple sites into the respective rabbits. The third immunization, given 3 months

later, contained 1 mg of hemocyanin, conjugated with either NAAG or NAA, in 1 ml of PBS. This solution was emulsified with 1 ml of Freund's incomplete adjuvant, and injected subcutaneously at multiple sites. This sequence of injections was maintained throughout the immunization regimen. Blood was collected from the rabbits 10–14 days after each injection and the serum was stored in 1 ml aliquots at −80° C.

*Affinity purification*

Antibodies to NAAG and NAA were purified in two stages, a primary affinity purification followed by pre-incubation with several immobilized protein-hapten conjugates (negative-affinity adsorption). The second step was required to remove remaining cross-reactivities to structurally similar molecules. Each affinity column was produced by rinsing 10 ml of aminoalkyl-agarose gel (Affi-gel 102, Bio-Rad; Norcross, CA) with 40 ml of deionized water and resuspending the agarose beads in 14 ml of water in polypropylene tubes. Thirty mg of either NAAG or NAA were added to the reaction tubes and the pH was adjusted to 5.5 with NaOH. Three hundred mg of EDAC were added to each tube, and the tubes were agitated by rotation for 1 h at room temperature. The affinity gels were washed with 50 ml of PBS and treated for 1 h with 4% NGS in PBS. Gels were then packed in 1 cm × 10 cm columns. One milliliter of each crude antiserum was diluted 50-fold in PBS containing 4% NGS and 0.1% sodium azide and filtered through a 0.45 μm syringe filter. Each solution was applied to its respective column, and the mixtures were continuously circulated in a loop with a peristaltic pump overnight at room temperature. The columns were then washed with 40 ml of PBS. Two milliliters of normal goat serum were added to each of the collection tubes before elution. The bound antibodies were eluted with 40 ml of 3 M magnesium chloride in PBS (pH 5.5), the eluates were dialyzed thoroughly against PBS, and the antibody solutions were stored at 4° C with 0.1% sodium azide.

*Negative-affinity adsorption*

Affinity purified antibodies were further purified by adsorption with nitrocelluose-immobilized protein-hapten conjugates and carbodiimide treated brain poteins. Conjugates were produced by coupling various small molecules to bovine serum albumin (BSA) with carbodiimide. NAAG antibody solutions were incubated overnight with 2–3 mg of NAA-BSA, 2 mg of GABA-BSA, and 1 mg each of glutamate-BSA, aspartate-BSA and N-acetylglutamate-BSA, as well as several mg of carbodiimide treated brain proteins adsorbed to nitrocellulose strips as previously described (Moffett *et al.*, 1994). The affinity purified NAA-antibodies required more extensive blocking, and were treated with 3–4 mg each of NAAG-BSA, glutamate-BSA, aspartate-BSA and GABA-BSA, 1–2 mg of taurine-BSA, 1 mg N-acetylglutamate-BSA and several mg of carbodiimide treated brain proteins. Affinity purified antibodies to NAAG and NAA, diluted 1 : 50 relative to the volume of crude serum, were preincubated with the immobilized conjugates overnight with constant rotary agitation at room temperature. The nitrocellulose strips were removed and the antibody solutions were filtered through 0.45 μm syringe filters and stored at 4° C with 0.1% sodium azide.

*Antibody characterization*

Solid phase immunoassays were performed with BSA-hapten conjugates spotted on nitrocellulolse sheets in a dilution series ranging from 2 μg to 1 ng of protein per spot. The compounds tested included BSA conjugates of NAAG, NAA, N-acetylglutamate, aspartate, glutamate, GABA, homocysteic acid, taurine and pyroglutamate. In addition, bovine skeletal muscle actin was tested with spots ranging from 1 μg to 0.5 ng. Sheets were air dried and treated with 4% NGS and 1% BSA in PBS for 1 h. Nitrocellulose sheets were then incubated overnight, with rotary agitation, in the standard working dilution of either primary antibody (1 : 250 for anti-NAAG and 1 : 1,000 for anti-NAA). The sheets were washed six times with PBS, and then incubated for 90 min with 10 ml of 1 μg $ml^{-1}$ HRP-labelled goat anti-rabbit secondary antibodies diluted in PBS containing 0.1% BSA. The sheets were washed six times with PBS and developed for 10 min with diaminiobenzidene and urea peroxide (Sigmafast tablets, Sigma).

*Immunohistochemistry*

Four male Long-Evans hooded and two male Sprague-Dawley albino rats (~ 150 gm, Zivic Miller; Zellenople, PA) were deeply anaesthetized with Nembutal (100 mg $kg^{-1}$). Each animal was perfused transcardially with 400 ml of a solution composed of 5 or 6% carbodiimide in deionized water containing 6% dimethylsulfoxide (DMSO), 1 mM N-hydroxysuccinimide, and heated to 37° C (Moffett *et al.*, 1993, 1994). One male albino rat, weighing 130 gm, was anaesthetized and perfused transcardially with 400 ml of a 4% solution of formaldehyde in PBS at pH 7.4 and 37° C. Brains were then fixed for 24 h in 100 mM sodium phosphate in physiological saline containing 4% formaldehyde at pH 8. The tissue was saturated in series with 10%, 20% and 30% sucrose solutions in PBS prior to freezing. Brains were sectioned in the frontal plane at a thickness of 20 μm, and the immunohistochemistry was performed in accordance with previous reports (Moffett *et al.* 1991a, 1993, 1994; Williamson *et al.* 1991).

Tissue sections were incubated at room temperature with 2% NGS in PBS containing 0.1% sodium azide for 30 min or longer. Affinity and adsorption purified anti-NAAG antibodies were diluted to a final concentration of 1 : 250 in the same solution (relative to the initial volume of rabbit serum). Sections were incubated for 24–48 h at room temperature under constant rotary agitation. Dual-purified antibodies to NAA were diluted 1 : 1000 in 2% NGS (relative to serum volume), and incubated with adjacent tissue sections under the same conditions. Some serial sections were incubated with polyclonal antibodies to the 67 kDa form of glutamic acid decarboxylase ($GAD_{67}$), one form of the enzyme which synthesizes GABA. The $GAD_{67}$ antibody (K2, purchased from Chemicon, Temecula CA) was diluted 1 : 12 000 in 2% NGS, and incubated with tissue sections under the same conditions. Forebrain tissue selections which had been fixed only with formaldehyde were incubated with standard antibody dilutions (1 : 250 NAAG, 1 : 1000 NAA), and with increased antibody concentrations (1 : 100 NAAG, 1 : 250 NAA), to verify that no protein immunoreactivity was being detected. Endogenous peroxidase activity was blocked in the formaldehyde fixed sections by incubating them for 30 min

in a 50:50 mixture of methanol and water containing 1% hydrogen peroxide. Bound antibodies were visualized by the avidin-biotin complex method with peroxidase as the marker enzyme. The biotinylated secondary antibodies and avidinated peroxidase solutions were each incubated with tissue sections for 70 min, with four washes of PBS between. After final washing, the sections were developed with a Ni and Co enhanced diaminobenzidene/peroxide reaction (Pierce Chemical Co., Rockford IL). The sections were mounted on Superfrost/plus slides (Fisher Scientific, Pittsburgh, PA), dried, dehydrated in an ethanol series, cleared in xylene and covered with resin.

*Antibody blocking with protein conjugates*

Antibody blocking studies with NAAG-BSA and NAA-BSA were done with the same nitrocellulose immobilized conjugates used for the second stage of purification. The two-stage purified anti-NAAG antibodies were diluted 1:250 in 2% NGS and separate aliquots were treated overnight with either 1, 2, 5, 10 or 20 $\mu g\,ml^{-1}$ of NAAG-BSA adsorbed to nitrocellulose, using constant rotary agitation. Additional aliquots of the same antibody preparation were incubated with 50, 100 and 200 $\mu g\,ml^{-1}$ of NAA-BSA under the same conditions. Glutamate-BSA and aspartate-BSA were incubated with two other aliquots of the same dilution of anti-NAAG antibody at a concentration of 200 $\mu g\,ml^{-1}$. A corresponding blocking study was performed with the two stage purified anti-NAA antibodies diluted 1:1000 in 2% NGS. Separate aliquots were treated overnight with various concentrations of several protein-hapten conjugates including 5, 10 or 20 $\mu g\,ml^{-1}$ of NAA-BSA, 50 or 100 $\mu g\,ml^{-1}$ of NAAG-BSA, or 200 $\mu g\,ml^{-1}$ of glutamate-BSA or aspartate-BSA.

## Results

*Specificity testing and pyramidal cell staining*

All rabbits produced specific antibodies to the protein-coupled hapten they were immunized with. The antibodies to NAAG from all three animals were more cross-reactive with protein-coupled NAA than any other tested conjugate. Variations were noted in the level of cross-reactivity in the antibodies produced in the three rabbits. The antibodies used in the present study were purified from the sera of the rabbit with the lowest degree of cross-reactivity. After initial affinity purification, these antibodies typically retained 25% cross-reactivity with NAA-BSA, and approximately 5% cross-reactivity with other conjugates including N-acetylglutamate-BSA, glutamate-BSA, GABA-BSA and aspartate-BSA, as estimated by binding to the antigen dilution series spotted on nitrocellulose sheets (Fig. 1A, upper left). Little or no cross-reactivity was observed with pyroglutamate, taurine, or homocysteic acid. Preincubation of the affinity purified antibodies with the protein conjugates described in Materials and Methods reduced all cross-reactivities, except that to NAA-BSA, to undetectable levels. Cross-reactivity with NAA-BSA after negative-affinity adsorption was typically reduced to approximately 1% as estimated by the staining intensities of serially diluted samples adsorbed to nitrocellulose sheets (Fig. 1A, upper right).

NAA antibodies were found to be approximately 5–10% cross-reactive with NAAG-BSA, N-acetylglutamate-BSA, aspartate-BSA and GABA-BSA after affinity purification (Fig. 1A, lower left). Treatment of the affinity preparation with the protein conjugates described above reduced cross-reactivity to all conjugates to extremely low ($\leqslant 0.25\%$) or undetectable levels except for NAAG-BSA and N-acetylglutamate-BSA, which remained approximately 5% cross-reactive (Fig. 1A, lower right). Both NAAG and NAA antibodies were tested for their ability to bind to bovine skeletal muscle actin. The dual-purified NAA antibodies did not cross-react to any degree with this isoform of actin. However, the dual purified antibodies to NAAG were able to clearly detect 50 ng of bovine skeletal muscle actin, and faintly detect 10 ng, on nitrocellulose sheets at the antibody dilution used for immunohistochemistry (data not shown).

Blocking studies with the dual purified anti-NAAG antibodies were used to compare the ability of protein conjugates of NAAG and NAA, adsorbed to nitrocellulose sheets, to inhibit the antibody binding to tissue sections. The NAAG antibody aliquots treated with 1 $\mu g\,ml^{-1}$ and 2 $\mu g\,ml^{-1}$ of NAAG-BSA had significantly attenuated signals. After treatment with 5 $\mu g\,ml^{-1}$ of NAAG-BSA, the primary NAAG antibody signal was greatly reduced. Only very slight NAAG-IR was observed in brain sections after the primary antibody was treated with 10 $\mu g\,ml^{-1}$ of NAAG-BSA, and at a concentration of 20 $\mu g\,ml^{-1}$, immunoreactivity in carbodiimide fixed brain sections was completely eliminated. In contrast, when the primary anti-NAAG antibodies were treated with 50 $\mu g\,ml^{-1}$ of NAA-BSA, no reduction was observed in NAAG-IR in serial sections. Pretreatment with 100 $\mu g\,ml^{-1}$ of NAA-BSA had only a very slight effect on NAAG-IR, and 200 $\mu g\,ml^{-1}$ reduced immunoreactivity further, but the reduction was far less than that observed with the antibody treated with 1 $\mu g\,ml^{-1}$ of NAAG-BSA. Glutamate-BSA and aspartate-BSA at 200 $\mu g\,ml^{-1}$ had no effect on NAAG-IR in carbodiimide fixed brain sections.

The blocking study performed with the two-stage purified anti-NAA antibodies yielded similar results, but demonstrated moderate cross-reactivity with protein-coupled NAAG. NAA-BSA at a concentration of 5 $\mu g\,ml^{-1}$ significantly reduced NAA-IR in carbodiimide-fixed brain tissue sections, and 10 $\mu g\,ml^{-1}$ reduced the immunoreactivity to very low levels. At a concentration of 20 $\mu g\,ml^{-1}$ of NAA-BSA, immunoreactivity for NAA was almost eliminated. NAAG-BSA was found to have a significant effect on

NAA-IR, such that at a concentration of $50\,\mu g\,ml^{-1}$, there was a noticeable reduction in the NAA signal. The signal was further reduced at a concentration of $100\,\mu g\,ml^{-1}$ NAAG-BSA, but the remaining NAA-IR was stronger than that observed after pretreatment with $5\,\mu g\,ml^{-1}$ of NAA-BSA. These values are in good agreement with the estimated 5% cross-reactivity of the anti-NAA antibodies to NAAG-BSA determined by solid-phase immunoassay. Protein conjugates of glutamate and aspartate at a concentration of $200\,\mu g\,ml^{-1}$ were found to reduce background staining, but had little or no effect on neutronal NAA-IR in tissue sections.

Immunohistochemistry of rat frontal cortex with affinity purified anti-NAAG antibodies that retained approximately 25% cross-reactivity with NAA-BSA is shown in Fig. 1B. Immunoreactivity with this affinity preparation was moderate in non-pyramidal neurons in all layers and in pyramidal neurons in layers II, III, V and VI as well. Staining with this antibody preparation was also observed in endothelia and pia, a characteristic of NAA-IR, rather than NAAG-IR (see below). After second-stage, negative affinity adsorption, the anti-NAAG antibodies stained non-pyramidal neurons in layers I–VI strongly, and only stained a small number of layer V pyramidal neurons lightly to moderately (Fig. 1C). The NAA-IR observed in rat neocortex with the two-stage purified-NAA antibodies was typically strong in pyramidal cells of layers II and V (Fig. 1D), and light to moderate in pyramidal cells in other layers, and non-pyramidal neurons in all layers.

*Immunohistochemistry*

The staining patterns observed for NAAG and NAA were consistent between animals in this and previous studies. Staining intensity was slightly variable between animals, apparently dependent upon the quality of the perfusion. The staining pattern for NAAG was much more regionally localized to specific cell groups, pathways, and terminal zones as compared with NAA, which was more widely distributed in rat forebrain, and more diffuse in the neuropil. In general, the pattern we observed with two-stage purified antibodies to NAA was very similar to the pattern described by Tsai and colleagues (1993) with their affinity purified antibodies to NAAG.

NAAG-IR in the present study was visible in neuronal somata external to cell nuclei, in basal and some distal dendritic branches, throughout the extent of axons, and in synaptic puncta ranging widely in size. NAA-IR was observed in neuronal somata and some dendrites, especially apical dendrites in pyramidal cells. NAA staining was also present in axonal projections such as the corpus callosum and corticospinal tracts, but was much less well defined than axonal NAAG-IR. NAA-IR in neurons was both diffuse and punctate in the cytoplasm, and was usually excluded from the cell nucleus. In some neurons, several large puncta were evident in the cytoplasm, and in some pyramidal cells, especially those of CA3 in hippocampus, one notably large spot of NAA-IR was observed, often at the base of the apical dendrite (see Fig. 4D, F). Moderate NAA-IR was observed in the pia mater, and in some ependymal cells. Also, a small number of capillary endothelial cells stained moderately to strongly with the highly purified NAA antibodies. However, based upon their appearance, this may have involved blood constituents coupled to the endothelium during carbodiimide fixation. Because NAA is derived predominantly or solely from the nervous system (Miyake *et al.*, 1981), these results could suggest that NAA is excreted into the blood stream, and that this normal excretion is elevated dramatically in Canavan disease (Hagenfeldt *et al.*, 1987; Matalon *et al.*, 1988). However, it is not clear whether the NAA-IR observed in endothelium, leptomeninges, ependymal cells and other surface structures was an artifact of the fixation method, due to insufficient antibody purification, or accurately represented high levels of NAA in these areas. The selective nature of the staining of some endothelial cells with this antibody preparation but not others, requires further investigation.

Formaldehyde fixation was used to determine if NAAG-IR or NAA-IR could be observed in the absence of the carbodiimide fixative. No NAAG-IR or NAA-IR was seen in brain tissue slices fixed only with formaldehyde at the antibody concentrations used for immunohistochemistry. When applied at four times its standard dilution (1:250), the NAA antibodies exhibited no significant binding to formaldehyde fixed sections. When applied at 2.5 times the standard dilution (1:100), the NAAG antibodies bound to a very slight degree with some blood or blood vessel elements, some pial and ependymal cells, and with small cells in the Islands of Calleja. Because little or no NAAG would be coupled to tissue proteins during the formaldehyde fixation, this slight immunoreactivity may have been due to cross-reactivity with proteins, such as actin. The level of immunoreactivity under these conditions was extremely low when compared to the specific signals observed in carbodiimide fixed tissue with more dilute antibody solutions.

*Primary sensory and motor cortices*

The comparative distribution of NAAG, $GAD_{67}$, and NAA immunoreactivities is shown in Fig. 2. NAAG-IR was observed predominantly in non-pyramidal neurons in layers I–VI in all isocortical regions (Fig. 2A). Fibres which were immunoreactive for NAAG were observed entering the cortex from the corpus callosum, most notably occurring in sensory areas. These

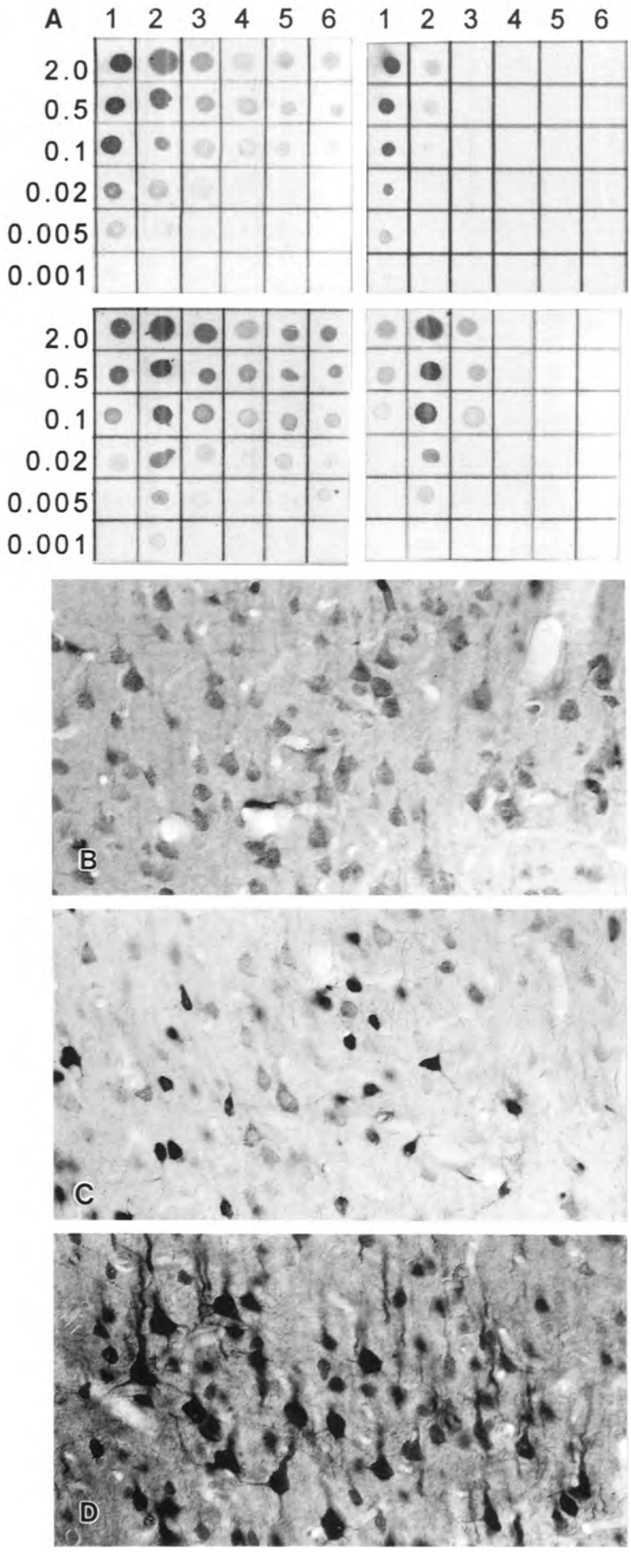
A
1 2 3 4 5 6
1 2 3 4 5 6
2.0
0.5
0.1
0.02
0.005
0.001
2.0
0.5
0.1
0.02
0.005
0.001
B
C
D

NAAG-IR fibres appeared to terminate mainly in layer IV. Very faint punctate staining of some pyramidal neurons was noted in layer V, and an occasional layer V pyramidal cell was stained moderately in certain regions, particularly in granular cortex. NAAG-IR neurons were relatively sparsely distributed in layer III of most neocortical regions (Fig. 3A), but relatively dense in layer IV of granular cortex (Fig. 3D). A similar arrangement was observed in serial sections stained with antibodies to $GAD_{67}$. Relatively sparse $GAD_{67}$-IR somata and puncta were observed in layer III, and this was particularly evident in motor cortex (Fig. 3B). However, in adjacent somatosensory cortex, layer IV contained numerous $GAD_{67}$-IR neurons, fibres and puncta (Fig. 3E). While the distribution and morphology of NAAG-IR and $GAD_{67}$-IR neuronal somata were the same, the number of $GAD_{67}$-IR fibres and puncta far exceeded those exhibiting NAAG-IR.

NAA-IR was strongest in pyramidal cells in isocortex, but was also observed in non-pyramidal neurons, e.g. layer IV cells of granular cortex (Fig. 2C). Pyramidal neurons of layers II and V were the most immunoreactive for NAA, and the apical dendrites of those in layer V could be observed in the overlying layers (Fig. 3C,F). It should be noted that this arrangement was similar to the observed staining pattern reported for NAAG by Tsai and colleagues (1993). Most neurons in layers III, IV and VI were lightly to moderately immunoreactive for NAA, but some neurons in layer VIb were strongly stained.

*Hippocampus*

NAAG-IR in the rat hippocampus was observed in non-pyramidal neurons, some with relatively large somata, in all layers of the hippocampus (Fig. 4A). In CA1, NAAG-IR neurons, many larger than pyramidal cells, were observed scattered through the pyramidal cell layer (Fig. 4C). Similar scattered, strongly NAAG-IR cells were also observed in CA2, CA3 (Fig. 4E) and the dentate gyrus. The greatest density of NAAG-IR neurons in the hippocampus was observed in the dentate gyrus, at the inner edge of the lateral blade granule cell layer. Their neuronal somata, situated in the polymorph layer, had NAAG-IR dendrites oriented through the granule cell layer which entered the molecular layer. Some of these neurons may have been basket cells. The precommissural hippocampus (tenia tecta) was characterized by a lack of staining in principle neurons of layer II, but strong NAAG-IR in medium to large non-pyramidal neurons within layers II, III and IV (Fig. 4G). A few scattered small cells were immunoreactive for NAAG in layer I. Numerous NAAG-IR fibres were observed coursing in a dorsoventral direction in the deep layers of the precommissural hippocampus.

NAA-IR was present in most or all pyramidal cells, polymorph cells and granule cells (Fig. 4B). Unlike NAAG-IR in the hippocampus, pyramidal cells in all regions were moderately to strongly stained for NAA (Fig. 4D,F). Also in contrast with NAAG staining, light to moderate NAA-IR was observed in many granule cells in the hippocampus, and these were most prevalent in the medial blade of the dentate gyrus. As with staining in neocortex, our two-stage purified anti-NAA antibodies produced a staining pattern similar to that reported for NAAG by Tsai and colleages (1993) with their affinity purified antibodies to NAAG. NAA-IR in the precommissural hippocampus was strong in all pyramidal cells of layer II, as well as many cells of the deeper layers (Fig. 4H).

*Anterior thalamus and retrosplenial cortex*

NAAG-IR in the anterior thalamic nuclei and retrosplenial cortex demonstrated a significant involvement of NAAG in specific portions of this thalamocortical projection. Strong NAAG-IR was observed in the neurons and neuropil of the anterodorsal thalamic nucleus (Fig. 5A). The neuropil staining for NAAG was more prominent at the anterior pole, while the strongest NAAG-IR in neurons was observed in the caudal portion of the nucleus. NAAG-IR was also observed in neurons of the anteroventral thalamic nucleus, predominantly in the dorsomedial subdivision (Fig. 5B). Punctate neuropil NAAG-IR was evident throughout the anteroventral thalamic nucleus, also being more dense dorsomedially than ventrolaterally. These nuclei are known to project largely to the superficial layers of retrosplenial granual cortex in the rat (Shibata, 1993). NAAG-IR in the retrosplenial granular cortex was observed in a population of fibres in the

**Fig. 1.** Antibody specificity and pyramidal cell staining. The solid phase immunoassay consisted of a serial dilution of various molecules, coupled to BSA and adsorbed to nitrocellulose, with a protein content ranging from 2 μg to 1 ng per spot (left column). Hapten-protein conjugates are numbered as follows (top row); (1) NAAG-BSA, (2) NAA-BSA, (3) N-acetylglutamate-BSA, (4) glutamate-BSA, (5) aspartate-BSA, and (6) GABA-BSA. Solid phase immunoassays are shown for several antibody preparations, including the first stage affinity purified anti-NAAG antibodies (A, upper left), affinity and absorption purified anti-NAAG antibodies (A, upper right), anti-NAA antibodies after affinity purification (A, lower left), and anti-NAA antibodies after affinity and adsorption purification (A, lower right). The first-stage, affinity purified anti-NAAG antibodies moderately stained pyramidal cells, non-pyramidal cells, and some endothelia in neocortex (layer V shown, B). Two-stage purified anti-NAAG antibodies predominantly stained non-pyramidal cells strongly in all cortical areas, and only stained some pyramidal cells lightly to moderately in neocortex (C). Two-stage purified NAA antibodies stained many pyramidal cells, as well as non-pyramidal cells in neocortex strongly (D). (B–D) ×216.

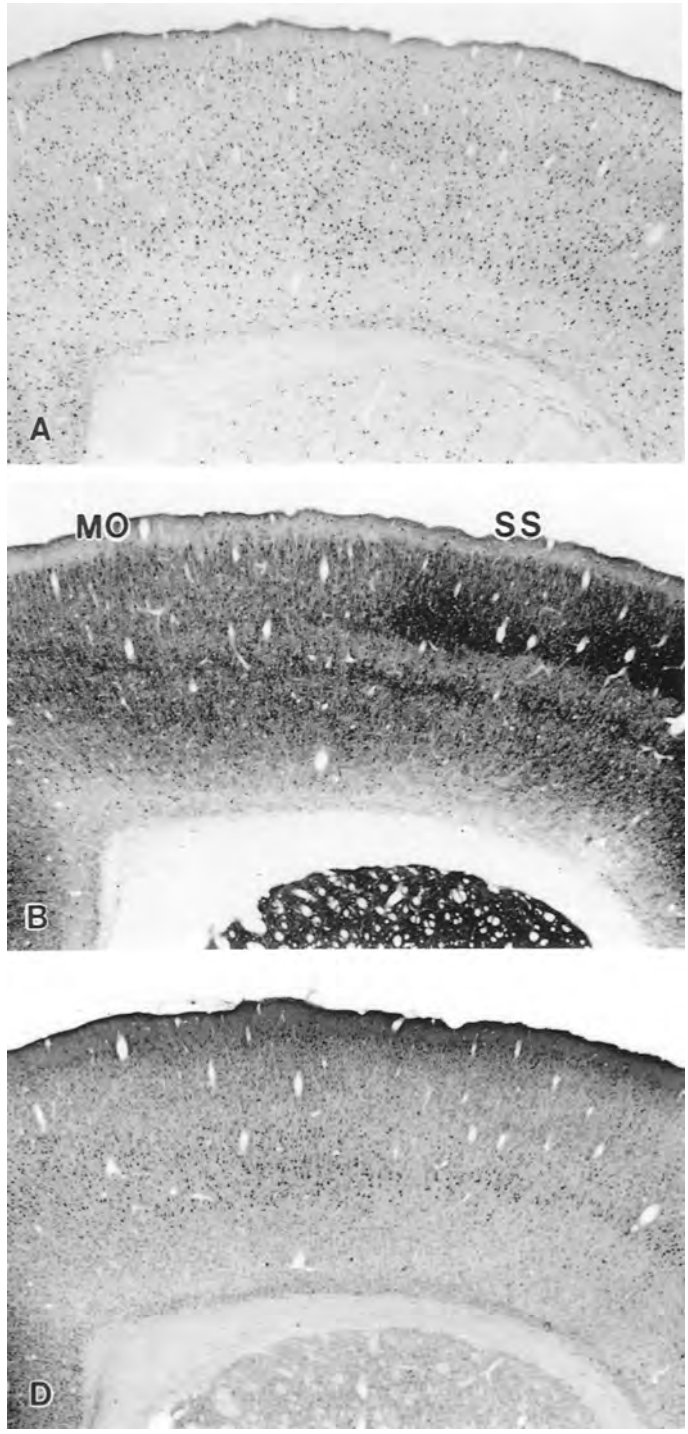


**Fig. 2.** NAAG, NAA and $GAD_{67}$ immunohistochemistry in serial sections of rat neocortex. Scattered non-pyramidal neurons were stained for NAAG in all cortical layers of neocortex (A). $GAD_{67}$-IR was observed in scattered interneurons, and in a complex network of fine processes and terminals in all cortical layers (B). Primary motor cortex (MO) can be seen to lack the dense layer of $GAD_{67}$-IR neurons, processes and puncta in layer IV of adjacent primary somatosensory cortex (SS). NAA-IR was present in most cortical neurons, and was most intense in pyramidal neurons of layers II and V (C). NAA-IR was also strong in the neuropil of the superficial layers of cortex. (Note: medial is to the left, and tissue slices are rotated counterclockwise approx. 15° in Figs 2 and 3). (A–C) ×22.

cingulum, which terminated relatively sparsely in layers IV and III, and very heavily in the superficial part of layer I (Fig. 5C,E). Many non-pyramidal neurons were strongly immunoreactive for NAAG in layers III–VI of retrosplenial granular cortex. NAAG-IR neurons appeared to be more numerous in layers III and V, with occasional layer V pyramidal neurons staining moderately to strongly. The distribution of

NAAG-IR observed in retrospenial granular cortex in the present investigation was very restricted when compared with that reported by Tsai and colleagues (1993).

NAA-IR was more widespread in the anterior thalamus than was NAAG-IR. Neuronal staining for NAA was strong in the anterodorsal thalamic nucleus, and moderate to strong throughout the anteroventral nucleus, anteromedial nucleus and mediodorsal nucleus (Fig. 5B). In retrosplenial granular cortex, NAA-IR was strong in pyramidal cells in layer V, in many smaller cells in layer III and IV, as well as in the neuropil of layer I (Fig. 5D,F). This distribution pattern observed for NAA-IR in retrosplenial cortex was similar to the pattern reported for NAAG by Tsai and colleagues (1993).

*Olfactory bulb and olfactory nuclei*

Strong immunoreactivity for NAAG was observed in many mitral cells in the rat olfactory bulb, as reported by Tsai and colleagues (1993). NAAG-IR in the present investigation was also very strong in periglomerular cells and apparent interneurons (Fig. 6A). No NAAG-IR was observed in the olfactory nerve. In the olfactory glomeruli, very fine fibres and puncta were moderately immunoreactive for NAAG. Periglomerular cells were among the most immunoreactive elements for NAAG in the olfactory bulb (Fig. 6A). NAAG-IR in the external plexiform layer consisted of fine calibre fibres, some small round cell somata, portions of some mitral cell dendrites, and a few widely scattered tufted cells. Light punctate NAAG staining was observed in the neuropil of the external plexiform layer, usually more pronounced in the inner half of the layer. Most mitral cells stained moderately to strongly for NAAG in their somata and variable portions of their dendrites, and the staining was conspicuously punctate, as reported by Tsai and colleagues (1993). The internal plexiform layer exhibited relatively low levels of NAAG-IR, which was observed in the somata of scattered interneurons, and in some vertically and horizontally oriented fibres. NAAG-IR in the internal granule layer was intense in large interneurons, and ranged from light to strong in a small subpopulation of internal granule cells. Numerous internal granule cells exhibited no immunoreactivity for NAAG, a finding in agreement with Tsai and colleagues (1993). The lateral olfactory tract contained many NAAG positive fibres, (Fig. 6C). NAAG-IR in accessory olfactory bulb was reduced in comparison with the main olfactory bulb, appearing light to moderate in the mitral cells and periglomerular cells. NAAG-IR in the anterior olfactory nucleus was almost indistinguishable from staining in the piriform cortex (Fig. 6E). Non-pyramidal neurons were highly immunoreactive throughout all subdivisions of the anterior olfactory nucleus. Numerous axons of the lateral olfactory tract were immunoreactive for NAAG, and punctate NAAG-IR was observed throughout the superficial molecular layer. In contrast to our observations, Tsai and colleagues (1993) reported strong NAAG-like immunoreactivity throughout the external plexiform layer, and in most tufted cells. They failed to detect significant NAAG-IR in periglomerula cells and interneurons of the internal granule cell layer, where we observed strong staining for NAAG.

NAA-IR in the rat olfactory bulb was observed in many neurons in all layers, but was not observed in the olfactory nerve fibres (Fig. 6B). Staining for NAA in the glomerular layer was most prominent in the distal dendrites of mitral cells, and in the dendrites of tufted cells. Most periglomerular cells were not

**Fig. 3.** Comparative distribution of NAAG, $GAD_{67}$, and NAA immunoreactivities in rat neocortex. This figure shows enlargements from Fig. 2 of primary motor cortex (top row) and primary somatosensory cortex (bottom row). NAAG-IR in primary motor cortex is shown in (A). $GAD_{67}$-IR and NAA-IR in serial sections of the same region are shown in (B) and (C) respectively. The distributions of NAAG-IR (D), $GAD_{67}$-IR (E), and NAA-IR (F) are compared in primary somatosensory cortex. Note that these sections correspond approximately to plate no. 14 from Swanson (1992). (A–F) ×72.

**Fig. 4.** NAAG-IR and NAA-IR in rat hippocampus. Immunoreactivity for NAAG was observed in scattered neurons, many with large somata, in all layers of the hippocampus, while NAA-IR was strong in pyramidal cells. These distinct immunohistochemical patterns are shown for CA1 (NAAG, C; NAA, D) and CA3 (NAAG, E; NAA, F). A similar arrangement was observed in the precommissural hippocampus (G, NAAG; H, NAA) where NAA-IR was particularly strong in pyramidal cells. Sections shown in (A–F) correspond approximately to plate no. 32, and sections in (G) and (H) to plate no. 12 (Swanson, 1992). (A,B) ×22; (C–F) ×216; (G,H) ×80.

**Fig. 5.** The anterior thalamus and retrosplenial cortex. Both neurons and neuropil were intensely stained for NAAG in the anterodorsal thalamic nucleus (AD in 5A; medial is to the left). In the anteroventral nucleus (AV), the dorsomedial division exhibited stronger neuronal NAAG-IR than the ventrolateral division. NAA-IR was strong in the AD and moderate in the AV (B). These thalamic nuclei project to the superficial layers of retrosplenial granular cortex (NAAG, C,E; NAA, D,F). The highest level of neuropil staining for both compounds was observed in the superficial part of layer I (asterisks, E and F). The stria terminalis (ST) was immunoreactive for NAA (B), but not for NAAG (A). Strong NAAG-IR was observed in the thalamic reticular nucleus (TR; A), where only light to moderate NAA-IR was observed (B). Medial is to the left in A and B, and to the right in (C–F). Sections correspond approximately to plates no. 26 (A,B) and no. 29 (C–F) (Swanson, 1992). (A,B) ×40; (C,D) ×80 (E,F) ×216.

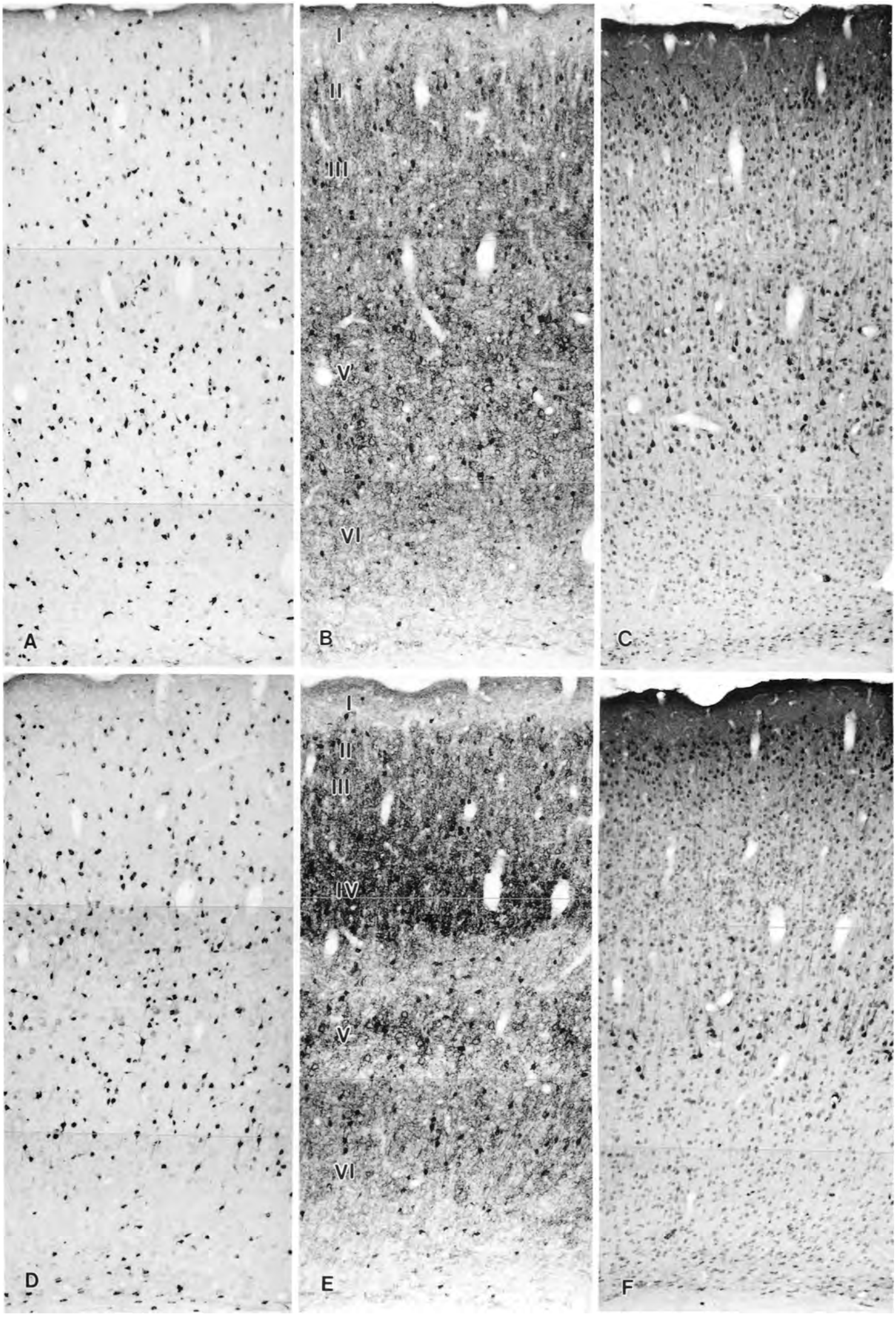
I
II
III
V
VI
A
B
C
I
II
III
IV
V
VI
D
E
F

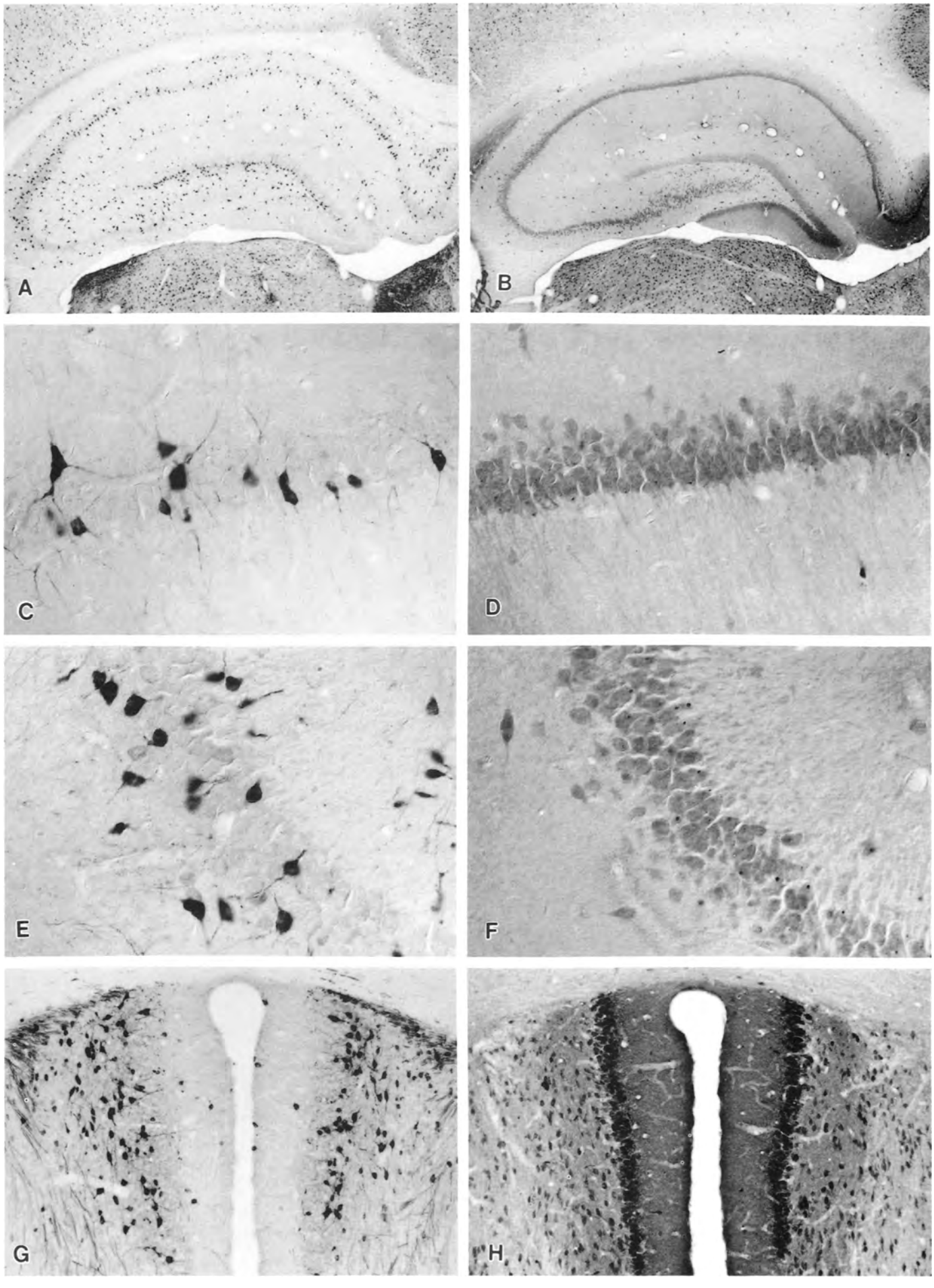
A
B
C
D
E
F
G
H

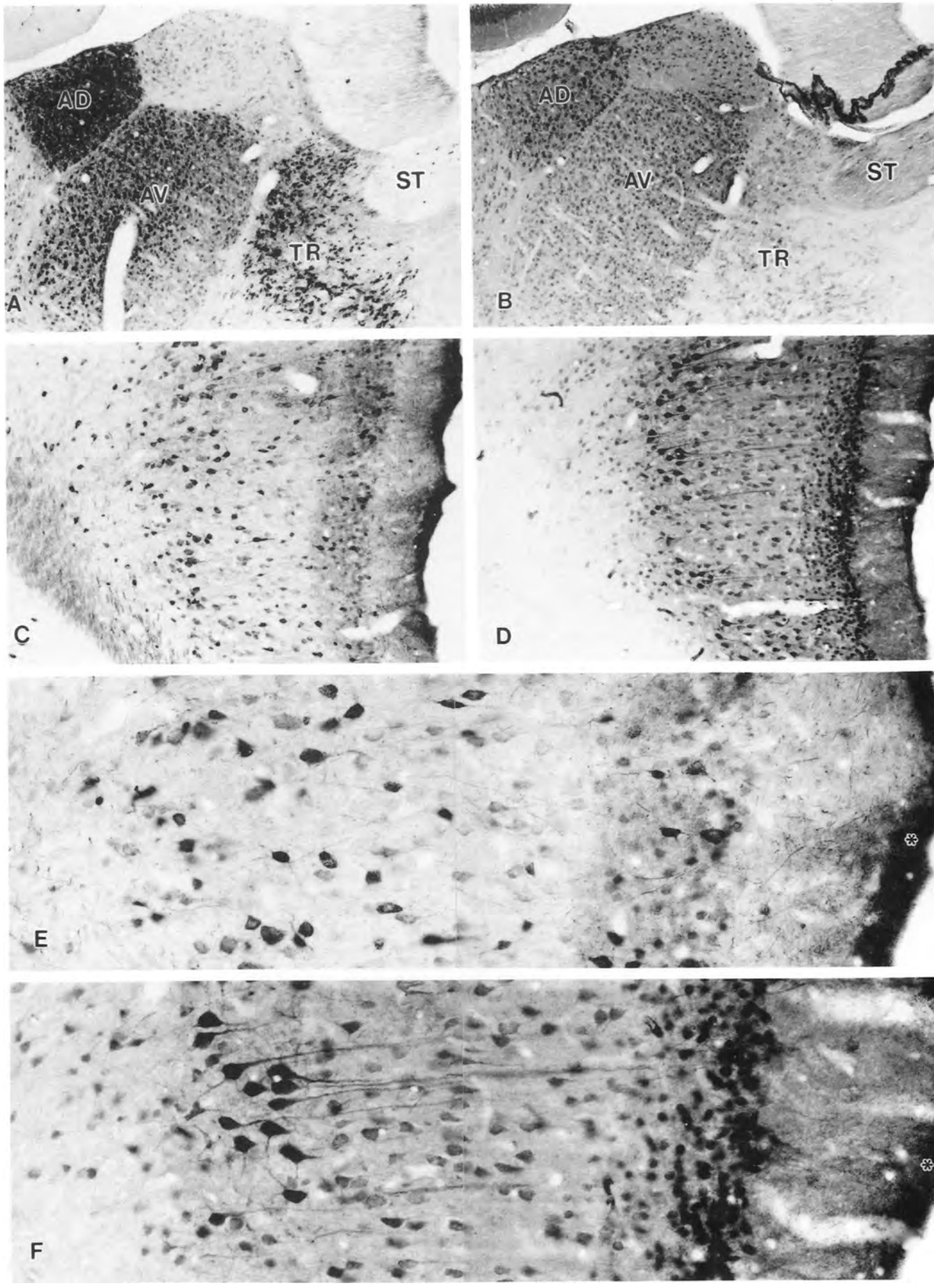
AD
AV
ST
TR
A
AD
AV
ST
TR
B
C
D
E
F

significantly immunoreactive for NAA, but some were moderately to strongly stained. NAA-IR in the external plexiform layer was strong, and was observed in neuronal processes and puncta within the neuropil. Numerous tufted cells were immunoreactive for NAA in the external plexiform layer. High levels of NAA-IR were observed in most mitral cells, which were immunoreactive in their cell bodies and portions of their dendritic arborizations. The internal plexiform layer was only lightly immunoreactive for NAA, where staining was observed in the axons of some mitral cells and in the somata of internal granule cells. The majority of internal granule cells in the olfactory bulb were lightly to moderately immunoreactive for NAA. The accessory olfactory bulb exhibited light to moderate NAA-IR, with relatively low levels present in the principal neurons (Fig. 6D). NAA-IR in all subdivisions of the anterior olfactory nucleus was consistent with the designation of this structure as a portion of the piriform cortex (Fig. 6F). Staining for NAA in the anterior olfactory nucleus was present predominantly in pyramidal cells in all regions. Moderate to strong NAA-IR was observed in numerous axons in the lateral olfactory tract. The distribution of NAA-IR observed in the present study was similar to the pattern reported for NAAG by Tsai and colleagues (1993; Fig. 6B).

*Piriform cortex, olfactory tubercle and hypothalamus*

NAAG-IR in piriform cortex was generally similar to that observed in other cortical regions, wherein apparent interneurons, many with relatively large somata, were strongly immunoreactive in all layers (Fig. 7A). Many axons of the lateral olfactory tract were moderately to strongly immunoreactive for NAAG. Fine-grained, densely packed, punctate NAAG staining was observed in the olfactory tract termination zone in layer Ia of piriform cortex. Lightly-stained NAAG-IR puncta were also evident in, or on layer II piriform pyramidal cells. A small number of widely scattered small round cells were immunoreactive for NAAG in layer II. Many endopiriform cells were strongly stained for NAAG (Fig. 7G). The olfactory tubercle had exceptionally low levels of NAAG-IR (Figs. 7A,E), except in the deeply situated islands of Calleja, where it ranged from moderate to strong (Fig. 7C). NAAG-IR in the accumbens nucleus was very sparse, and consisted of widely scattered small and medium sized neurons (Fig. 7A). Some fibres in the olfactory limb of the anterior commissure were immunoreactive for NAAG, but many appeared unstained. Numerous hypothalamic areas contained strong NAAG-IR in neurons, fibres and puncta, including the magnocellular preoptic nucleus (Fig. 7E). The level of NAAG-IR in the hypothalamus was higher than most other forebrain regions.

NAA-IR in piriform cortex was strong in most or all of the pyramidal cells of layer II, an observation reported by Tsai and colleagues (1993) with their affinity purified antibodies to NAAG. (Fig. 7B). We observed additional neurons immunoreactive for NAA scattered in layers I and III. Most endopiriform neurons were moderately stained for NAA (Fig. 7H). The lateral olfactory tract contained numerous NAA-IR fibres. Immunoreactivity for NAA in the olfactory tubercle was strong in cells of layer II (Fig. 7F). NAA-IR was only light in the deeply situated islands of Calleja, but was strong in the more superficially situated islands external to layer II in the tubercle (Fig. 7B,D). In the accumbens nucleus, NAA-IR was light in most neurons (Fig. 7B). Only light NAA-IR was observed in the anterior commissure. Many regions of the hypothalamus contained neurons which were strongly stained for NAA, similar to the pattern observed for NAAG, but with less immunoreactivity in the neuropil (Fig. 7F).

*The septum and nucleus of the diagonal band*

Like the hypothalamus, several nuclei in the septal region exhibited some of the highest levels of neuronal NAAG-IR in the rat forebrain. Most or all neurons in the medial septum and both limbs of the nucleus of the diagonal band of Broca were intensely immunoreactive for NAAG. These nculei were similar in appearance in NAAG stained sections (Fig. 8A,C). Both cholinergic neurons and GABAergic neurons are present in these cell groups, (Gritti *et al.*, 1993), so it remains to be determined if NAAG-IR is colocalized with one or both of these neurotransmitters in this region. The lateral septum, however, contained only very few widely scattered NAAG-IR neurons (Fig. 8C). In contrast to these results, Tsai and colleagues (1993) reported moderate NAAG-IR in neurons of the medial and lateral septum.

Moderate to strong NAA-IR was observed in many neurons of the nucleus of the diagonal band (Fig. 8B). NAA-IR was light to moderate in most neurons of the septal nuclei, with the neurons of the medial septum exhibiting stronger neuronal NAA-IR (Fig. 8D).

*Extrapyramidal system*

The NAAG-IR observed in the rat extrapyramidal system under the present conditions was consistent with a previous description (Moffett *et al.*, 1989), but much greater detail was afforded by the newer methods. NAAG staining in the caudoputamen was observed in scattered neurons with small round, or medium sized fusiform and triangular somata, and in a population of axons in the penetrating fascicles of the internal capsule (Fig. 9A,C). Portions of the dendritic arborizations of the NAAG-IR striatal neurons exhibited a characteristic beaded appearance. In our previous study, and in Tsai and colleages (1993), the details of the NAAG-IR in these neurons, as well as the

population of NAAG-IR fibres in the internal capsule, were not observed. In the globus pallidus (Fig. 9A), ventral pallidum and entopeduncular nucleus (Fig. 9G), most medium and large neurons and portions of their dendrites were strongly immunoreactive for NAAG. In the neuropil, a characteristic pattern of dense punctate staining was observed in all subdivisions of the pallidum, as reported by Tsai and colleagues (1993) (Fig. 9E).

NAA-IR in the rat striatum was observed in most neurons in the caudoputamen (Fig. 9B). It ranged from light to strong in neuronal somata, but the processes of striatal neurons did not stain for NAA (Fig. 9D). NAA-IR in the rat pallidum was light to moderate in many neurons, somewhat similar to the pattern observed for NAAG, but with lower intensity and less NAA-IR present in the neuropil (Fig. 9B,F). The entopeduncular nucleus was similar in appearance to other portions of the pallidum in NAA stained sections (Fig. 9H).

*Anterior amygdala*

While Tsai and colleagues (1993) reported little or no NAAG-IR in the rat amygdala, we observed strongly stained scattered neurons in every subdivision (Fig. 10A,C). The areas with the highest number of NAAG-IR cells included subdivisions of the central nuclei, particularly the medial division, where most neurons were immunoreactive. The basolateral nucleus contained relatively few NAAG-IR neurons in comparison. The remaining subdivisions of the amygdala contained a population of strongly NAAG-IR neurons similar to allocortical structures such as as the piriform cortex.

In contrast, NAA-IR in the amygdala was light to moderate in most of the neurons in all subdivisions. The basolateral amygdaloid nuclei exhibited stronger NAA-IR than other subdivisions, unlike the case with NAAG-IR (Fig. 10B,D). Light to moderate NAA-IR was observed in the central nuclei, and moderate to strong NAA-IR was observed in neurons of the cortical amygdaloid area.

*Other NAAG-IR forebrain regions*

The habenula displayed a specific immunoreactivity pattern for NAAG. Extremely strong cellular and neuropil NAAG-IR was observed in the lateral habenula, while a network of more moderately stained NAAG-IR fibres and puncta were present in the medial subdivision, where no neurons contained NAAG-IR (Fig. 11A). NAAG-IR was very strong in the ascending fibres of the medial lemniscus, as reported previously (Moffett *et al.* 1994). These NAAG-IR fibres entered the ventrobasal thalamus to terminate in a dense plexus of nerve fibres and puncta (Fig. 11C,E). The neurons of the ventral posterolateral and ventral posteromedial nuclei were moderately to strongly stained for NAAG. Numerous other telencephalic and diencephalic areas contained notably high levels of NAAG-IR. Among these were the thalamic reticular nuclei, which expressed very strong NAAG-IR, an observation that supports colocalization with GABA (Fig. 11C). In accord with previous reports (Moffett *et al.* 1990,1991b), the most intense NAAG-IR in a major axonal projection was observed in the optic nerves, chiasm and tracts in the rat (see Fig. 10C).

The habenula also exhibited a specific distribution pattern for NAA-IR (Fig. 11B). The medial subdivision contained moderate staining in the neuropil, but no immunoreactivity in neurons. Neurons throughout the lateral subdivision contained moderate to strong NAA-IR. NAA-IR was light in the medial lemniscus, and moderate in the neurons of the ventral posterolateral and ventral posteromedial nuclei (Fig. 11D,F). Immunoreactivity for NAA was relatively light in the neurons of the thalamic reticular nucleus (Figs. 5B,11D).

## Discussion

Methodological differences in small molecule immunohistochemistry can lead to significant differences in the observed staining patterns. Antibody production and purification methods, as well as tissue fixation techniques, are important determining factors in the reliability of the immunohistochemical results. Polyclonal antibodies produced against small molecules coupled to proteins often exhibit numerous cross-reactivities, and require substantial purification to increase their specificity. Careful use of control experiments will provide a certain degree of confidence in the specificity of the purified antibodies. The importance of removing cross-reactive antibodies, and using positive and negative controls in the form of solid-phase immunoassays and antibody blocking studies has been emphasized by some of the pioneering researchers in the field of small molecule immunohistochemistry (Ottersen *et al.*, 1986). The procedures we have adopted in the present and previous investigations (Moffett *et al.*, 1993,1994) follow these guidelines. In a much earlier investigation we used procedures similar to those of Tsai and colleagues (1993), with prolonged postfixations in carbodiimide and antibodies to NAAG that were affinity purified, but not preadsorbed with NAA conjugates. Under these conditions, we observed the same strong pyramidal cell staining in rat cortex (Moffett *et al.*, 1989). By preadsorbing the affinity purified antibodies to NAAG with protein conjugates of NAA, and monitoring the level of cross-reactivity to NAA-BSA and other conjugates with solid-phase immunoassays, we have observed a much more restricted distribution of NAAG-IR in the rat forebrain than that reported by Tsai and colleagues (1993). Specifically, we observed NAAG-IR to be low or

absent in most cortical and hippocampal pyramidal neurons and granule cells. In addition, we have used differential blocking studies with serial dilutions of NAAG-BSA and NAA-BSA in parallel with our immunohistochemistry to provide greater confidence in the specificity of our antibody preparations.

Using the described methods, we found the immunoreactivity patterns for NAAG and NAA in the rat forebrain to be distinct, and consistent with two previous reports (Moffett *et al.*, 1991a,1993). The staining pattern observed with the single-step, affinity purified NAAG antibodies (shown in Fig. 2B) exhibited high background staining, and appeared to combine some aspects of the staining patterns observed with the two-step purified antibodies to NAAG (Fig. 2C) and NAA (Fig. 2D). Appreciable differentiation of the two immunohistochemical signals was dependent upon reducing the cross-reactivity of each antibody preparation to the other compound to low levels by negative-affinity adsorption. Overall, the greatest single problem with NAAG immunohistochemistry was attributable to antibody cross-reactivity with NAA-protein conjugates. The affinity purified anti-NAAG antibodies used by Tsai and colleagues (1993) were reported to have a cross-reactivity with protein conjugates of NAA of 42% (Blakeley *et al.*, 1987). The concentration of NAA is over 25 times higher than that of NAAG in the rat forebrain (9.19 vs 0.35 $\mu mol\,g^{-1}$ tissue respectively; Miyake *et al.*, 1981). Under such conditions, the degree of cross-reactivity between the anti-NAAG antibodies and protein-coupled NAA is critical. This concern has been noted by Blakely and Coyle (1988). Affinity purification of polyclonal antisera to NAAG will retain all antibodies with high affinity for NAAG, including those with cross-reactivities to other epitopes, such as protein-coupled NAA. In the present investigation, negative-affinity adsorption of the anti-NAAG antibodies with NAA coupled to BSA was found to be of critical importance in removing the remaining cross-reactive antibodies. After negative-affinity adsorption, it was found that treatment of the anti-NAAG antibodies with 1 $\mu g\,ml^{-1}$ of NAAG-BSA resulted in a greater reduction of NAAG-IR in carbodiimide fixed brain sections than did 200 $\mu g\,ml^{-1}$ of NAA-BSA. Immunohistochemistry with anti-NAAG antibodies which had been exhaustively blocked with NAA-BSA resulted in strong staining of non-pyramidal neurons, and little or no NAAG-IR in cortical and hippocampal pyramidal neurons.

In the present study, the faint, punctate staining of some pyramidal neurons with the two-stage purified anti-NAAG antibodies may have been due to the low (~1%) cross-reactivity with protein-coupled NAA. It is

**Fig. 6.** The olfactory bulb and olfactory nuclei (see Results section for description). NAAG-IR and NAA-IR are compared in the main olfactory bulb ((A) and (B) respectively). Immunoreactivity for NAAG and NAA are shown in the accessory olfactory bulb ((C) and (D) respectively) and anterior olfactory nucleus ((E) and (F) respectively). Medial is to the left in (C) and (D), and to the right in (E) and (F). Abbreviations: AOB, accessory olfactory bulb; AON, anterior olfactory nucleus; EPL, external plexiform layer; G, glomerular layer; IGL, internal granule cell layer; IPL, inner-plexiform layer; LOT, lateral olfactory tract; ON, olfactory nerve; MCL, mitral cell layer. (A,B) ×216; (C, D) ×22; (E,F) ×40.

**Fig. 7.** Piriform cortex, olfactory tubercle and hypothalamus. NAAG-IR was observed in the lateral olfactory tract (arrowhead in A), in the neuropil of layer Ia, in scattered cells in all layers (A), and in the deep endopiriform (DE) cortex (G). NAA-IR was observed in the lateral olfactory tract (arrowhead in B), in most neurons of layers II and III, and in neurons of the deep endopiriform cortex (B) and (H). NAAG-IR was very sparse in the accumbens nucleus (AC), but was strong in both small and medium sized cells of the islands of Calleja and the surrounding neuropil (C). NAA-IR levels were low in the deeper islands of Calleja when compared with NAAG (D). The number of NAAG-IR neurons was also very low in the olfactory tubercle (T), but very high in the adjacent magnocellular preoptic nucleus (MA) of the hypothalamus (E). NAA-IR was strong in the olfactory tubercle and the magnocellular preoptic nucleus (F). Sections correspond approximately to plates no. 11 (A–D) and no. 19 (E–H) (Swanson, 1992). (A,B) ×22; (C,D) ×80; (E–H) ×40.

**Fig. 8.** The septum and nucleus of the diagonal band. NAAG-IR was intense in many of the neurons of the nucleus of the diagonal band of Broca (A) and the medial septal nucleus (C). However, NAAG-IR was observed only in very few scattered neurons in the lateral septum (C). Neuronal NAA-IR was moderate to strong in the nucleus of the diagonal band (B) and the medial septal nucleus (D). Sections correspond approximately to plates no. 15 (A,B) and no. 16 (C,D) (Swanson, 1992) (A,B) ×40; (B,C) ×22.

**Fig. 9.** The striatum, pallidum and entopeduncular nucleus. NAAG-IR (A) was distinctly different in the striatum (caudoputamen; CP) and globus pallidus (GP). In contrast, NAA-IR did not delineate the striatum from the palidum, but was light to moderate in most neurons (B). Scattered small and medium sized neurons were strongly stained for NAAG in the striatum, as was a population of fibres in the internal capsule (C). Most of the small neurons in the caudoputamen were immunoreactive for NAA, but NAA immunoreactive fibres were not observed in the fascicles of the internal capsule (D). Very strong NAAG-IR was present in the neurons and neuropil of all subdivisions of the pallidum, including the globus pallidus (E), the ventral pallidum (substantia innominata), and the entopeduncular nucleus (G). NAA-IR was also observed in the neurons and the neuropil of the globus pallidus (F), ventral pallidum and entopeduncular nucleus (H), but fibres were poorly labelled. Sections correspond approximately to plate no. 25 (Swanson, 1992). (A,B,G,H) ×80; (C–F) ×216.

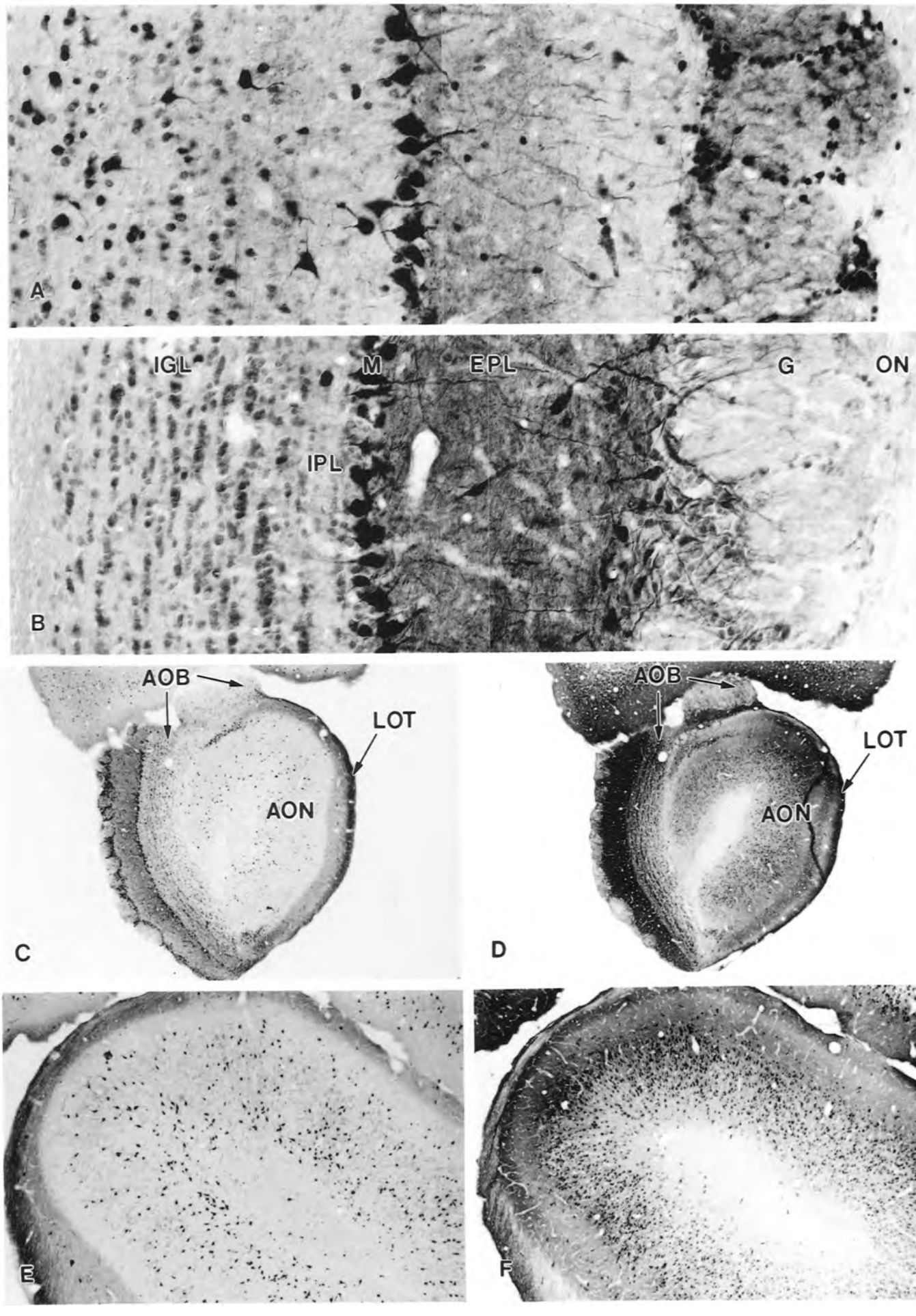
A
IGL
M
EPL
G
ON
IPL
B
AOB
LOT
AON
C
AOB
LOT
AON
D
E
F

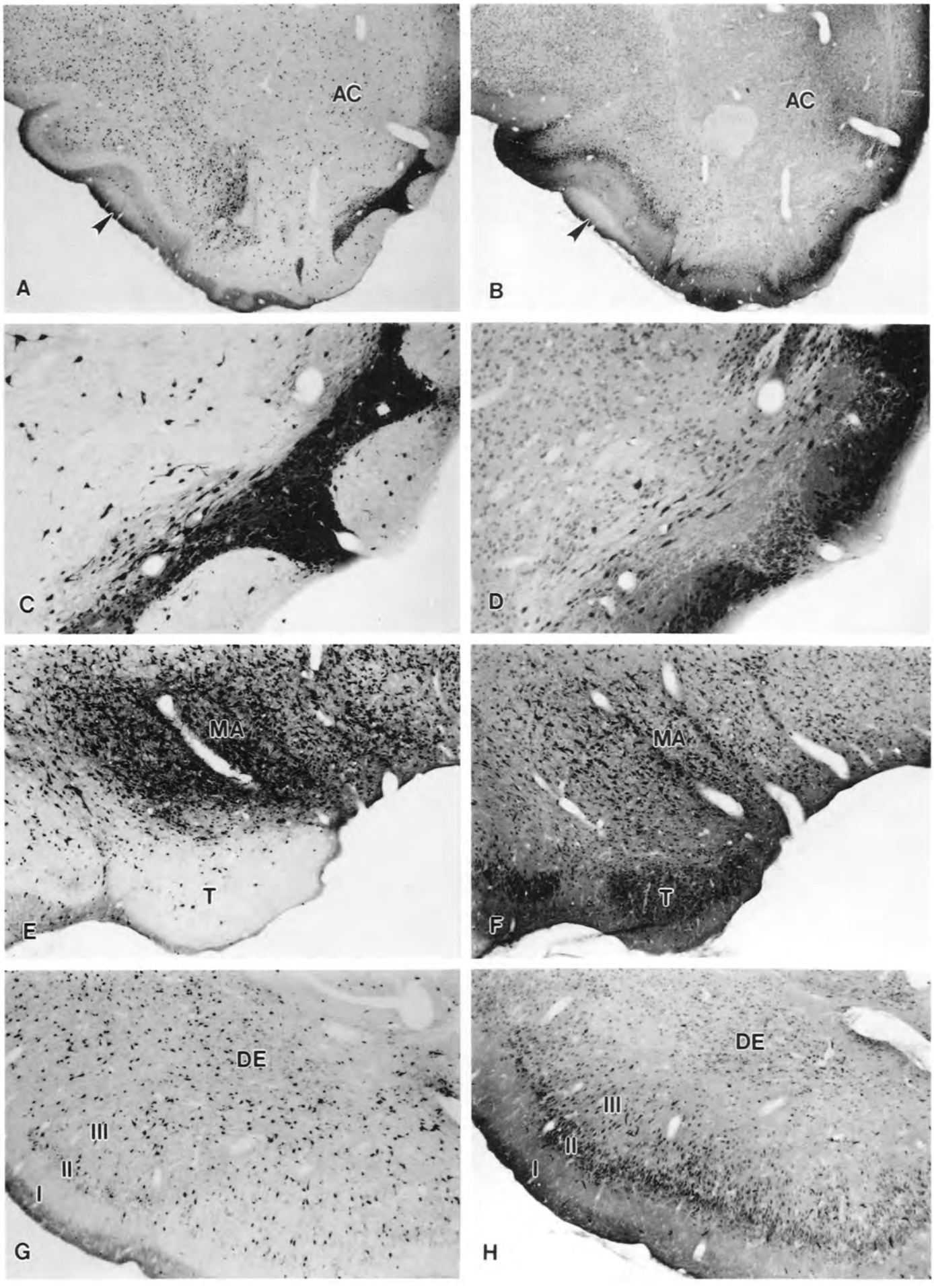
AC
A
AC
B
C
D
MA
T
E
MA
T
F
DE
III
II
I
G
DE
III
II
I
H

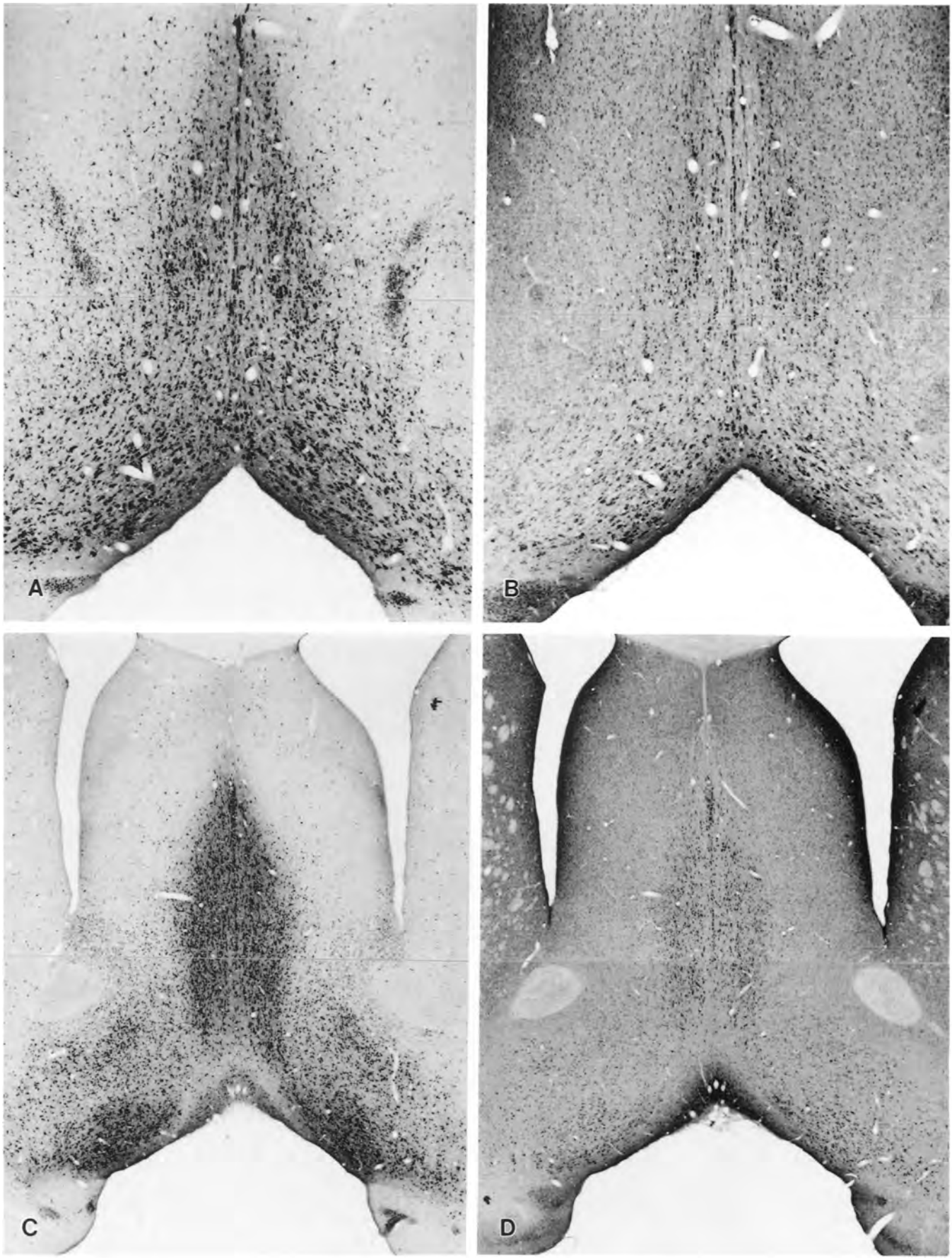
A
B
C
D

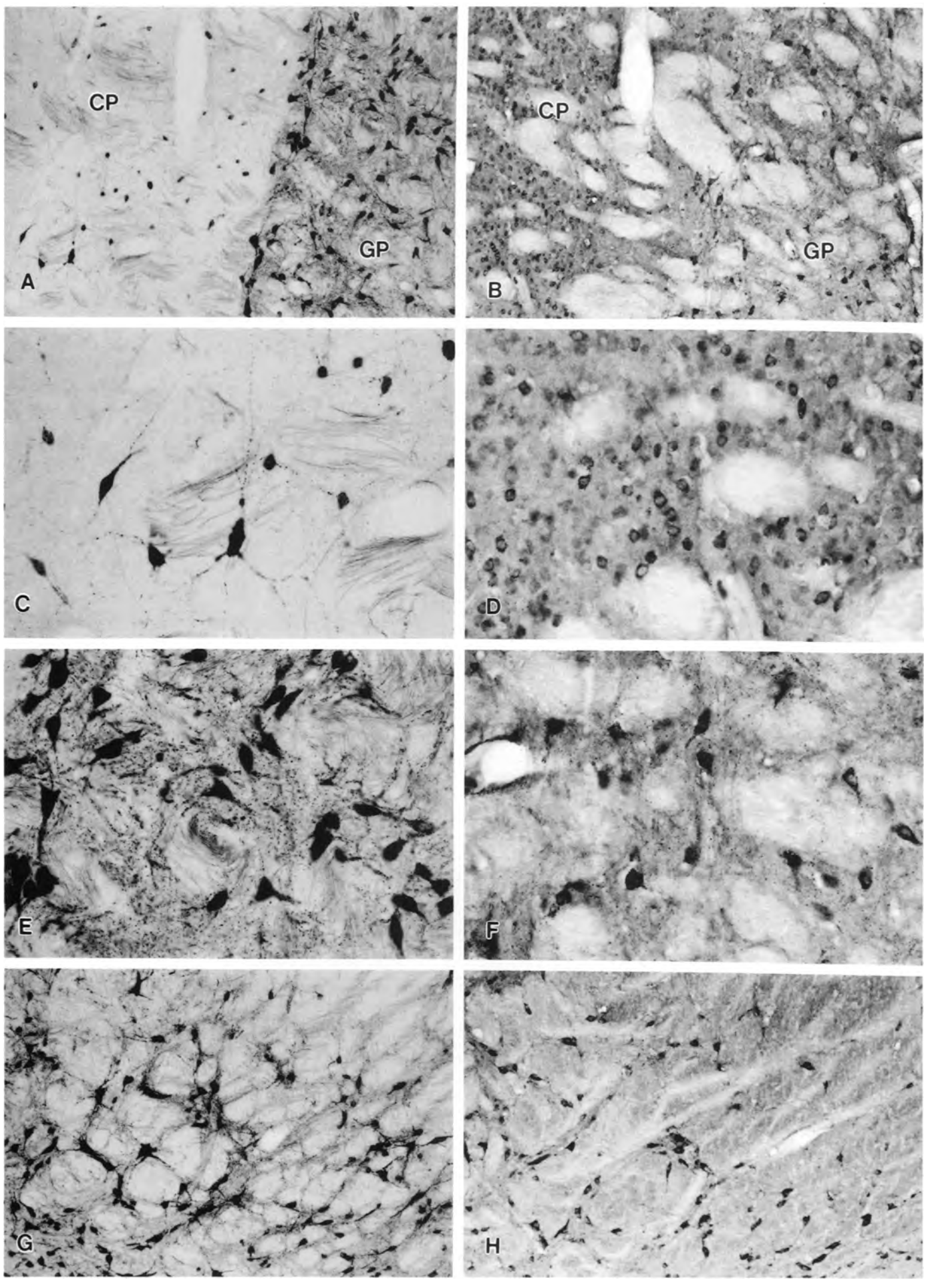
CP
GP
A
CP
GP
B
C
D
E
F
G
H

noteworthy that the cells exhibiting this faint NAAG-IR were in the same cortical regions that contained the most intense NAA-IR neurons. However, several factors argue against this interpretation. First, the size and distribution of the NAAG-IR puncta in pyramidal cells was different from that associated with NAA-IR. The NAAG-IR puncta observed in pyramidal cells were small, numerous, and distributed evenly throughout the cytoplasm. The NAA-IR puncta associated with pyramidal cells were fewer in number, larger in size, and often located sporadically in the cytoplasm (see Fig. 4F). These findings are suggestive of different intracellular compartmentation of NAAG and NAA, a possibility in need of further investigation. Second, very high levels of antibody blocking with protein-coupled NAA ($200\,\mu g\,ml^{-1}$) did not eliminate the light to moderate NAAG-IR observed in some pyramidal cells. Together, these two findings suggest that the relatively low NAAG-IR observed in some pyramidal neurons did reflect low levels of the dipeptide in these cells. Nonetheless, the faint staining of some pyramidal cells observed in cortical structures, whether due to the presence of low levels of NAAG, or cross-reactivity with high levels of NAA, represented a minor signal in rat cortex and hippocampus when compared to the staining observed in non-pyramidal neurons. In this context, it is noteworthy that species differences in NAAG levels have been reported (Miyake *et al.*, 1981), but not well studied. HPLC analysis of different microdissected regions of the rat and cat brain have shown large interspecific differences in NAAG concentration in several brain regions. For example, NAAG levels in the medial substantia nigra were $7.9 \pm 0.2\,nmol\,mg^{-1}$ protein and $56.7 \pm 5.2\,nmol\,mg^{-1}$ protein in the rat and cat respectively (Galli *et al.*, 1991). Similarly, immunohistochemical studies have demonstrated many pyramidal cells in the cortex of cats and monkeys do exhibit strong NAAG-IR (Tieman *et al.*, 1987,1991), contrasting with the absence, or faint immunoreactivity observed in the rat. We have confirmed these findings with two-stage purified anti-NAAG antibodies (unpublished observations), and are currently investigating the species differences in neocortical NAAG-IR levels.

Carbodiimide fixation is required to perform immunohistochemistry of small molecules which contain carboxyl groups and lack primary amine groups. A previous analysis of the parameters of carbodiimide fixation indicated that effective coupling of small molecules to proteins was dependent upon several factors (Moffett *et al.*, 1993). These included the elimination of buffers such as phosphate, because they increase the non-productive hydrolysis of carbodiimide and greatly reduce the coupling efficiency. In addition, carbodiimide mediated amide bond formation was found to be highly temperature sensitive such that fixations performed at 37° C, instead of room temperature, provided significantly greater signal. Perhaps the most important factor for improving carbodiimide based fixations was the use of DMSO to increase carbodiimide penetration into tissues. Greatly improved staining was observed in deep structures and fibre pathways when DMSO was included in the perfusion medium, but the use of DMSO did not affect NAAG-IR in cortical structures. Additionally, extended postfixations similar to those used by Tsai and colleages (1993) were found to produce edge artifacts including increased staining in cortex, which was accompanied by reduced or absent staining in central thalamus and cerebellum (Moffett *et al.*, 1993). In this regard, using the older fixation method, or the prolonged postfixation method used by Tsai and colleagues (1993) only weak NAAG-IR, or no NAAG-IR was observed in the ventrobasal thalamus (Henderson & Salt, 1988; Tsai *et al.*, 1993). However, due to the use of DMSO as a fixative penetrant in the present study, extensive NAAG staining was seen in the medial lemniscus, and in fibres, terminals and neurons throughout the ventrobasal thalamus.

Due to the identical structure of NAA and the N-terminus of NAAG, it is interesting that the purified NAA antibodies could distinguish between protein-coupled NAAG and NAA. Because most of the free primary amine groups in tissue proteins are contributed by lysine residues, a carbodiimide reaction involving NAAG and NAA would predominantly generate N-acetyl-aspartyl-glutamyl-lysine and N-acetyl-aspartyl-lysine moieties respectively. If the purified antibodes bind preferentially to these larger epitopes, then it would be possible for them to discriminate between the distinct peptide sequences produced by the coupling reaction. The NAAG antibodies were found to cross-react with bovine skeletal muscle actin, which is known to have NAAG at its N-terminus (Vandekerckhove & Weber, 1978). However, the N-terminal NAAG moiety in skeletal muscle actin is followed by acidic amino acids in the polypeptide chain, rather than lysine. Therefore, the fact that the two-stage purified NAAG antibodies did recognize this isoform of actin does not support the idea that they require the protein attachment site for their specificity. Conversely, the antibodies to NAA did not detect a spot containing as much as 1 μg of skeletal muscle actin. This finding, and the low cross-reactivity of the dual purified anti-NAA antibodies to NAAG-BSA, support the possibility that the NAA antibodies do bind to the larger peptide sequence involving the protein attachment site. It was considered possible that the antibodies to NAA would cross-react with the β isoform of brain actin, which contains NAA, rather than NAAG, at its N-terminus (Vandekerckhove & Weber, 1978). For this reason, formaldehyde perfusions were used to fix

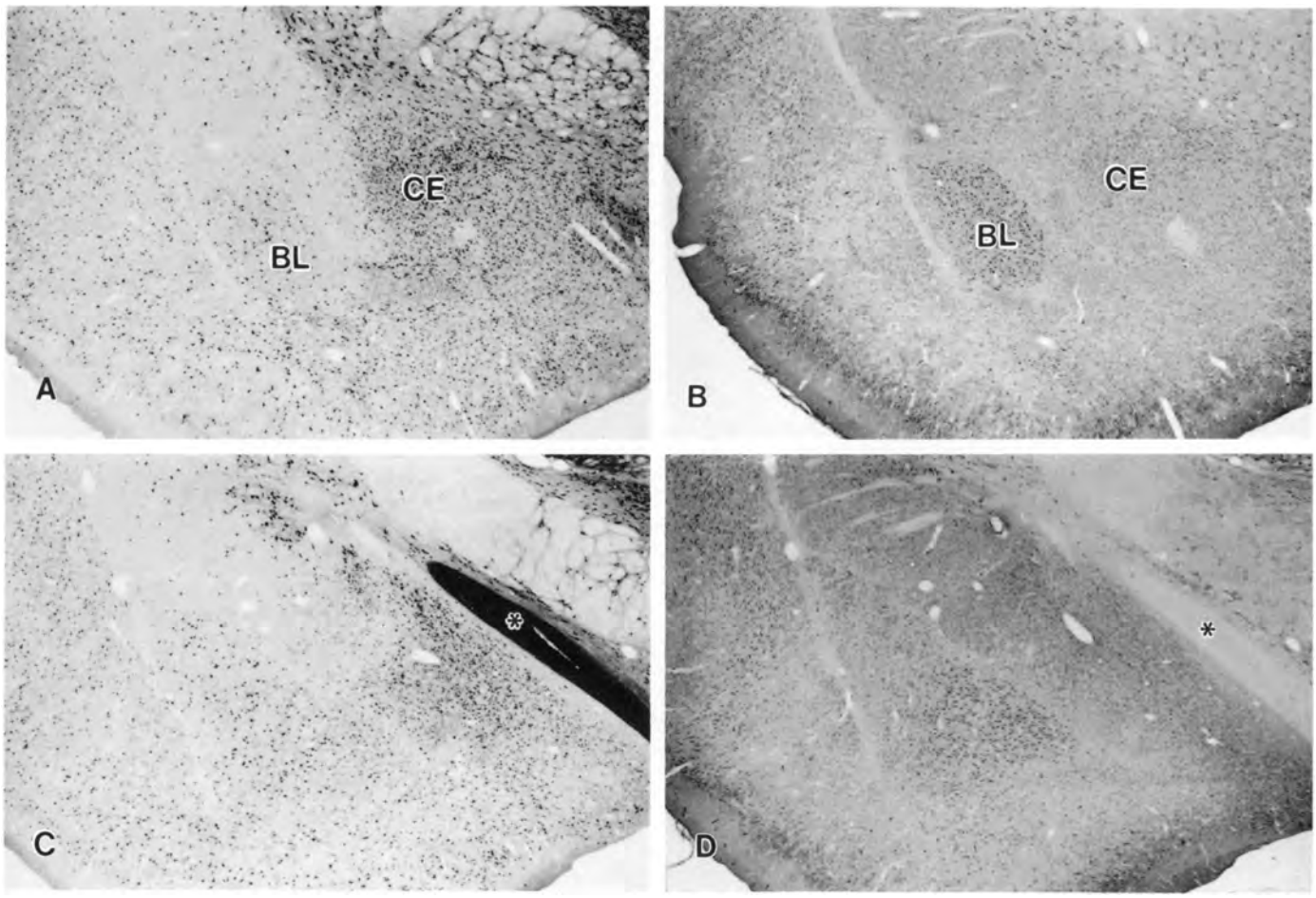


**Fig. 10.** NAAG and NAA immunoreactivities in the anterior amygdala. Scattered NAAG-IR neurons were observed in all divisions of the rat amygdala, with the highest numbers present in the medial part of the central nucleus (CE). NAA-IR was notably high in most neurons of the basolateral nucleus (BL). (C) and (D) show slightly more caudal levels of the amygdala. The optic tract is visible in (C) and (D) (asterisks). Sections correspond approximately to plates no. 27 and no. 28 (Swanson, 1992). (A–D) ×22.

tissue in the absence of carbodiimide, such that little or no NAAG and NAA would be coupled to tissue constituents. Under these conditions, no NAA-IR or NAAG-IR were observed in brain with antibodies at the dilutions used for immunohistochemistry. When the antibodies to NAA were applied to formaldehyde fixed tissue at four times the concentration used for immunohistochemistry, no significant immunoreactivity was observed. These results indicate that the NAA staining observed in neurons, glia, and certain blood vessel elements in carbodiimide fixed tissue was not due to cross-reactivity with actin or other proteins. This might relate to the fact that acidic amino acids are present in the polypeptide chain after the N-acetylaspartate terminus in β-actin (Vandekerckhove & Weber, 1978), rather than the lysine residue expected when NAA is coupled to proteins with carbodiimide. The lack of staining of the brain isoform of actin in formaldehyde fixed tissue further supports the possibility that the purified antibodies to NAA interact with the lysine attachment site of NAA-protein conjugates.

The results of the present study emphasize the importance of evaluating and minimizing cross-reactivity to structurally similar molecules when performing small molecule immunohistochemistry. In the case of the anti-NAAG antibody's cross-reactivity with protein-coupled NAA, the problem of structural similarity is exacerbated by the large differential in concentration of these two molecules in the rat forebrain. The delineation of the two immunohistochemical signals, made possible with dual positive-negative affinity purification of the antibodies, highlights the distinct cellular distribution patterns occupied by these two molecules. In this, and previous investigations (Moffett *et al.*, 1991a,1993), the distribution patterns observed were consistent with a significant colocalization of NAAG with GABA, and NAA with many transmitters notably including glutamate and aspartate, in the rat forebrain.

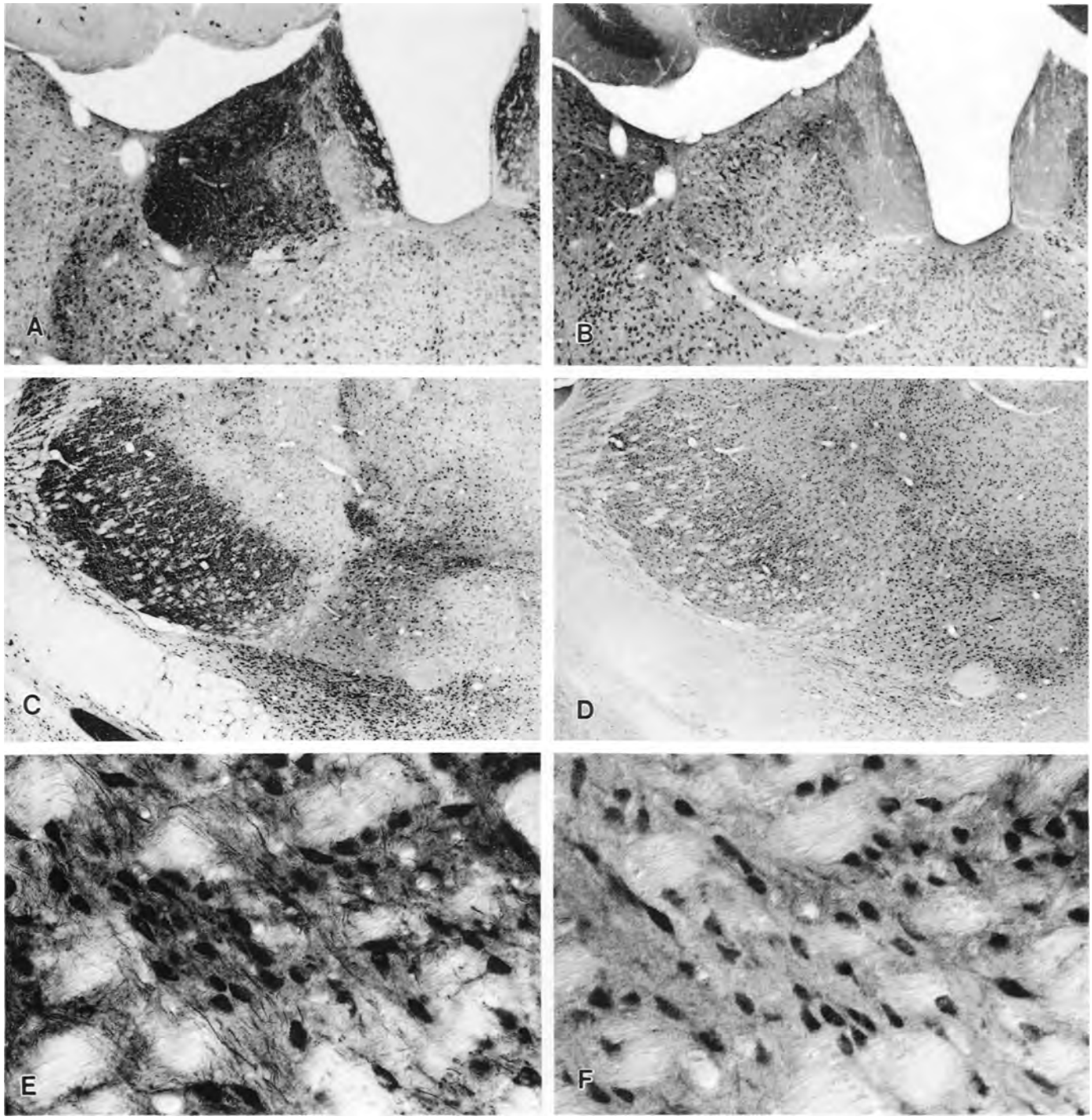


**Fig. 11.** Other NAAG-IR areas in rat forebrain. NAAG-IR was very pronounced in the neurons and neuropil of the lateral habenula, and the neuropil only in the medial habenula (A). Immunoreactivity for NAA was moderate to strong in the cells of the lateral habenula, and moderate in the neuropil of the medial habenula (B). NAAG-IR in the medial lemniscus and ventrobasal thalamus was very strong in both the afferent axons and the principal neurons, forming a semicircle of intense immunoreactivity in the lateral thalamus (C). Lemniscal afferents which were strongly NAAG-IR were visible entering the ventral posterolateral thalamic nucleus, where the somata of the principal neurons were also strongly stained (E). NAA-IR was observed in the principal neurons of ventrobasal thalamus, but not in the afferents from the medial lemniscus (D). The somata of ventrobasal neurons were strongly stained for NAA, but fibre labelling was poor (F). Sections correspond approximately to plate no. 32 from (Swanson, 1992). (A,B) ×40; (C,D) ×22; (E,F)×216.

NAAG-IR in forebrain was also observed in several glutamatergic and numerous cholinergic systems. While Tsai and colleagues (1993) only detected faint NAAG immunoreactivity in small neurons in the rat striatum, we observed a population of scattered small to medium sized neurons with varicose processes which were very strongly stained for NAAG in the striatum, and it is possible that these represented the cholinergic neurons of this region (Fig. 9C). Interestingly, in the rat hindbrain, NAAG-IR has been observed in numerous excitatory pathways, but not in most known GABAergic neurons (Moffett *et al.*, 1994). This apparent discrepancy in NAAG colocalization with excitatory vs inhibitory systems in the hindbrain and forebrain requires further investigation (see below). The relatively ubiquitous distribution pattern observed for NAA was not suggestive of a neurotransmitter role for this compound, but rather implicates NAA in metabolic, transport or storage functions in many neurons, especially large projection neurons as observed by Simmons and colleagues (1991). It is important to note that the overall lack of significant variation in NAA concentrations between different brain regions as shown by HPLC analysis (Koller *et al.*, 1984) belies its high levels in specific neurons, and relative paucity in others. NAA was not found to be distributed homogeneously in the brain, but rather, the level appeared to be highly variable among different neuronal types. Also, in many regions of the rat forebrain, the distributions of NAAG and NAA immunoreactivities were quite disparate, suggesting unrelated functions. It has been reported previously, on the basis of HPLC analysis of extracts from various regions of the CNS, that NAAG and NAA levels correlate poorly (Koller *et al.*, 1984).

The apparently extensive colocalization of NAAG with GABA in the rat forebrain is notable in that NAAG has been considered an excitatory transmitter candidate, rather than an inhibitory transmission modulator. The present results also indicate a possible heterogeneity among granule cells in the olfactory bulb, where only small subpopulations were significantly immunoreactive for NAAG. Interpretation of such results is further confounded by the extensive localization of NAAG in the optic projections, and in excitatory projection systems in the rat hindbrain (Moffett *et al.*, 1994). A noteworthy feature of NAAG immunoreactivity in the rat forebrain was that it was not typically observed in the axons or synaptic terminals of many GABAergic neurons. For example, neurons of the globus pallidus, and portions of their dendrites contained NAAG-IR, but the projection pathways which stained heavily for $GAD_{67}$ contained far fewer NAAG-IR axons (data not shown). Also, the distribution of $GAD_{67}$-IR neuronal somata and NAAG-IR neurons in neocortex was found to be virtually identical, but the dense fibre and terminal plexus that was stained for $GAD_{67}$ was not stained for NAAG. It is possible that colchicine treatment would permit visualization in these fibres, but this remains to be determined. In the present study, however, many probable GABAergic neurons contained NAAG in their somata and portions of their dendritic arborizations, but not in their axons or axon terminals. In contrast, when NAAG-IR was associated with excitatory systems, such as the optic projections (Moffett *et al.*, 1991b), or the mossy fibre projections to the cerebellar cortex (Moffett *et al.*, 1994), NAAG-IR was expressed at high levels in the axons and synaptic terminals. One hypothesis consistent with these observations is that NAAG can be excitatory at postsynaptic NMDA receptors, or modulate the release of a variety of transmitters at presynaptic sites, perhaps through presynaptic NMDA or metabotropic glutamate receptors. Thus, it is possible that NAAG may be released from synaptic terminals in excitatory pathways such as the primary visual projections, or from dendrites in GABAergic neurons to presynaptically alter further GABA release (Perouansky & Grantyn, 1990). In this regard, it is noteworthy that NAAG, which has been found in the cell bodies and dendrites of substantia nigra neurons (Moffett *et al.*, 1989), has also been reported to affect the release of dopamine from dendrites in the substantia nigra (Galli *et al.*, 1991). Potential interactions between NAAG and GABA remain a subject for future investigations. In conclusion, the discrete localization of NAAG and NAA in different neuronal populations should help guide further research into the diverse functions served by these ubiquitous brain compounds.

## Acknowledgments

This work supported by NIH Grant EY09085. Special thanks to Dr Joseph H. Neale for all of his help and support.

## References

BAUMINGER, S. & WILCHEK, M. (1980) The use of carbodiimides in the preparation of immunizing conjugates. *Methods in Enzymology* **70**, 151–9.

BIRKEN, D. L. & OLDENDORF, W. H. (1989) N-acetyl-L-aspartic acid: a literature review of a compound prominent in 1H-NMR spectroscopic studies of brain. *Neuroscience and Biobehavioural Reviews* **13**, 23–31.

BLAKELY, R. D. & COYLE, J. T. (1988). The neurobiology of

N-acetylaspartylglutamate. *International Review of Neurobiology* **30**, 39–100.

GALLI, T., GODEHEU, G., ARTAUD, F., DESCE, J. M., PITTALUGA, A., BARBEITO, L., GLOWINSKI, J. & CHËRAMY, A. (1991) Specific role of N-acetyl-aspartylglutamate in the in vivo regulation of dopamine release from dendrites and nerve terminals of nigrostriatal dopaminergic neurons in the cat. *Neuroscience* **42**, 19–28.

GOODFRIEND, T. L., LEVINE, L. & FASMAN, G. D. (1964) Antibodies to bradykinin and angiotensin: a use of carbodiimides in immunology. *Science* **144**, 1344–6.

GRITTI, I., MAINVILLE, L. & JONES, J. E. (1993) Codistribution of GABA—with acetylcholine-synthesizing neurons in the basal forebrain of the rat. *Journal of Comparative Neurology* **329**, 438–57.

HAGENFELDT, L., BOLLGREN, I. & VENIZELOS, N. (1987) N-acetylaspartic aciduria due to aspartoacylase deficiency — a new aetiology of childhood leukodystrophy. *Journal of Inherited Metabolic Disease* **10**, 135–41.

HENDERSON, Z. & SALT, T. E. (1988) The effects of N-acetylaspartylgutamate and distribution of N-acetyl-aspartylglutamate-like immunoreactivity in the rat somatosensory thalamus. *Neuroscience* **25**, 899–906.

KENDALL, P. A., POLAK, J. M. & PEARSE, A. G. (1971) Carbodiimide fixation for immunohistochemistry: observations on the fixation of polypeptide hormones. *Experientia* **27**, 1104–6.

KOLLER, K. J., ZACZEK, R. & COYLE, J. T. (1984) N-acetyl-aspartyl-glutamate: regional levels in rat brain and the effects of brain lesions as determined by a new HPLC method. *Journal of Neurochemistry* **43**, 1136–42.

MATALON, R., MICHALS, K., SEBESTA, D., DEANCHING, M., GASHKOFF, P. & CASANOVA, J. (1988) Aspartoacylase deficiency and N-acetylaspartic aciduria in patients with canavan disease. *American Journal of Medical Genetics* **29**, 463–71.

MIYAKE, M., KAKIMOTO, Y. & SORIMACHI, M. (1981) A gas chromatographic method for the determination of N-acetyl-L-aspartic acid, N-acetyl-aspartylglutamic acid and beta-citryl-L-glutamic acid and their distributions in the brain and other organs of various species of animals. *Journal of Neurochemistry* **36**, 804–10.

MOFFETT, J. R., CASSIDY, M. & NAMBOODIRI, M. A. (1989) Selective distribution of N-acetylaspartylglutamate immunoreactivity in the extrapyramidal system of the rat. *Brain Research* **494**, 255–66.

MOFFETT, J. R., NAMBOODIRI, M. A. & NEALE, J. H. (1993) Enhanced carbodiimide fixation for immunohistochemistry: application to the comparative distribution of N-acetylaspartylglutamate and N-acetylaspartate immunoreactivities in rat brain. *Journal of Histochemistry and Cytochemistry* **41**, 559–70.

MOFFETT, J. R., WILLIAMSON, L. C., PALKOVITS, M. & NAMBOODIRI, M. A. (1990) N-acetylaspartylglutamate: a transmitter candidate for the retinohypothalamic tract. *Proceedings of the National Academy of Sciences (USA)* **87**, 8065–9.

MOFFETT, J. R., NAMBOODIRI, M. A., CANGRO, C. B. & NEALE, J. H. (1991a) Immunohistochemical localization of N-acetylaspartate in rat brain. *Neuroreport* **2**, 131–4.

MOFFETT, J. R., WILLIAMSON, L. C., NEALE, J. H. PALKOVITS, M. & NAMBOODIRI, M. A. (1991b) Effect of optic nerve transection on N-acetylaspartylglutamate immunoreactivity in the primary and accessory optic projection systems in the rat. *Brain Research* **538**, 86–94.

MOFFETT, J. R., PALKOVITS, M., NAMBOODIRI, M. A. & NEALE, J. H. (1994) Comparative distribution of N-acetylaspartylglutamate and $GAD_{67}$ immunoreactivities in the cerebellum and precerebellar nuclei of the rat utilizing enhanced carbodiimide fixation and immunohistochemistry. *Journal of Comparative Neurology* **347**, 598–618.

OTTERSEN, O. P., STORM-MATHISEN, J. MADSEN, S., SKUMLIEN, S. & STRØMHAUG, J. (1986) Evaluation of the immunocytochemical method for amino acids. *Medical Biology* **64**, 147–58.

PEROUANSKY, M. & GRANTYN, R. (1990) Is GABA release modulated by presynaptic excitatory amino acid receptors? *Neuroscience Letters* **113**, 292–7.

PUTTFARCKEN, P. S., HANDEN, J. S., MONTGOMERY, D. T., COYLE, J. T. & WERLING, L. L. (1993) N-acetyl-aspartylglutamate modulation of N-methyl-D-aspartate-stimulated [$^3$H]norepinephrine release from rat hippocampal slices. *Journal of Pharmacology and Experimental Therapeutics* **266**, 796–803.

SEKIGUCHI, M., WADA, K. & WENTHOLD, R. J. (1992) N-acetylaspartylglutamate acts as an agonist upon homomeric NMDA receptor (NMDAR1) expressed in *Xenopus* oocytes. *FEBS Letters* **311**, 285–9.

SHIBATA, H. (1993) Efferent projections from the anterior thalamic nuclei to the cingulate cortex in the rat. *Journal of Comparative Neurology* **330**, 533–42.

SHIOSAKA, S., KIYAMA, H., WANAKA, A. & TOHYAMA, M. (1986) A new method for producing a specific and high titre antibody against glutamate using colloidal gold as a carrier. *Brain Research* **382**, 399–403.

SIMMONS, M. L., FRONDOZA, C. G. & COYLE, J. T. (1991) Imunocytochemical localization of N-acetyl-aspartate with monoclonal antibodies. *Neuroscience* **45**, 37–45.

SWANSON, L. W. (1992) *Brain maps: structure of the rat brain.* Elsevier: Amsterdam.

TIEMAN, S. B., CANGRO, C. B. & NEALE, J. H. (1987) N-acetylaspartylglutamate immunoreactivity in neurons of the cat's visual system. *Brain Research* **420**, 188–93.

TIEMAN, S. B., NEALE, J. H. & TIEMAN, D. G. (1991) N-acetylaspartylglutamate immunoreactivity in neurons of the monkey's visual pathway. *Journal of Comparative Neurology* **313**, 45–64.

TSAI, G., SLUSHER, B. S., SIM, L. & COYLE, J. T. (1993) Immunocytochemical distribution of N-acetylaspartylglutamate in the rat forebrain and glutamatergic pathways. *Journal of Chemical Neuroanatomy* **6**, 277–92.

VANDEKERCKHOVE, J. & WEBER, K. (1978) Mammalian cytoplasmic actins are the products of at least two genes and differ in primary structure in at least 25 identified positions from skeletal muscle actins. *Proceedings of the National Academy of Sciences (USA)* **75**, 1106–10.

WESTBROOK, G. L., MAYER, M. L., NAMBOODIRI, M. A. & NEALE, J. H. (1986) High concentrations of N-acetylaspartylglutamate (NAAG) selectively activate NMDA receptors on mouse spinal cord neurons in cell culture. *Journal of Neuroscience* **6**, 3385–92.

WILLIAMSON, L. C., EAGLES, D. A., BRADY, M. J., MOFFETT, J. R., NAMBOODIRI, M. A. & NEALE, J. H.

(1991) Localization and synaptic release of N-acetylaspartylglutamate in the chick retina and optic tectum. *European Journal of Neuroscience* **3**, 441–51.

WILLINGHAM, M. C. & YAMADA, S. S. (1979) Development of a new primary fixative for electron microscopic immunocytochemical localization of intracellular antigens in cultured cells. *Journal of Histochemistry and Cytochemistry* **27**, 947–60.